ANL-6634
Instruments
(TID-4500, 18th Ed.)
AEC Research and
Development Report

ARGONNE NATIONAL LABORATORY
9700 South Cass Avenue
Argonne, Illinois

TUNNEL DIODE CIRCUIT ANALYSIS

by

Ronald G. Roddick

Electronics Division

October 1962

Operated by The University of Chicago
under
Contract W-31-109-eng-38
with the
U. S. Atomic Energy Commission

DISCLAIMER

TABLE OF CONTENTS

LIST OF FIGURES

LIST OF FIGURES

LIST OF FIGURES

TUNNEL DIODE CIRCUIT ANALYSIS

by

Ronald G . Roddick

ABSTRACT

Several graphical and graphico-analytical methods for solving nonlinear differential equations are analyzed and used in the solution of the most common configurations for tunnel diode circuits. The general procedure is to perform a first integration in the phase plane and then obtain the time-dependent solutions by a second graphical integration.

The operating modes and stability of tunnel diode circuits are analyzed, and a useful parameter diagram is presented. Examples are analyzed in connection with the different methods.

Though tunnel diode circuits may be solved by means of an electronic computer, it is believed that these simple and easily applied methods give a valuable insight into the behavior of circuits under various operating conditions.

1. Introduction

Electronic circuits have been successfully studied with systems of linear differential equations serving as a mathematical model. These equations have been the subject of intense study, and the existence of well-known forms of solutions is now established. Their use depends upon the assumption that the circuit elements can be described by certain constant parameters. One example of this is the equivalent circuit of a triode, with the amplification factor and the plate resistance as constant parameters.

A cursory examination of the tunnel diode characteristics shows that it is an element that cannot be so easily "linearized." This is especially true when it is used as a switching element.

We have made an attempt to apply certain techniques for solving nonlinear differential equations to the specific case of solving tunnel diode circuits.

The tunnel diode equivalent circuit is shown in Fig. 1.0-1, in which N is a nonlinear element with the characteristic shown in Fig. 1.0-2.[10]

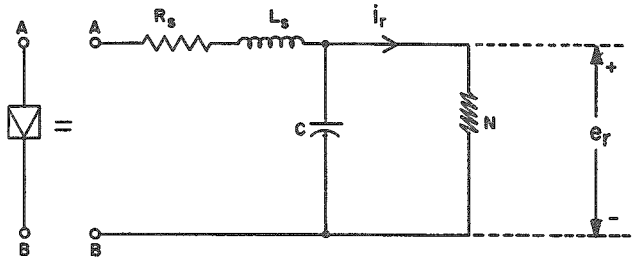

Fig. 1.0-1
Equivalent circuit for tunnel diode.

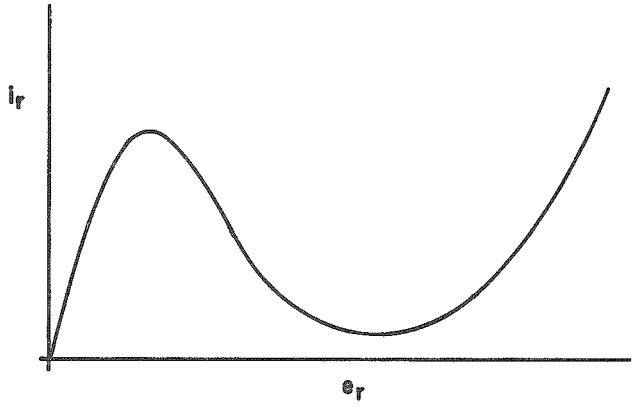

Fig. 1.0-2
i_r-e_r characteristic of tunnel diode.

Experience shows that for some applications resistance R_s and impedance L_s may be neglected in the analysis. In this case, we have the simplest possible circuit (Fig. 1.0-3). Sections 2.1.1 and 2.1.2 contain methods for analyzing this circuit.

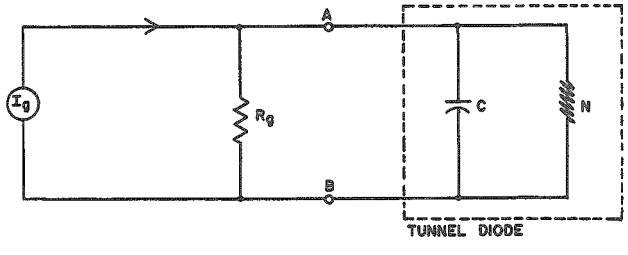

Fig. 1.0-3
The simplest tunnel diode circuit: one reactive element.

If we neglect only R_s and suppose the existence of an external generator with zero or pure inductive impedance, we have the circuit of Fig. 1.0-4. This case is treated by means of the isocline method in Section 2.2, and could be analyzed with the Lienard method,(2) (see Section 2.3). The Lienard method was invented for solving equations of the sort involved in this case.

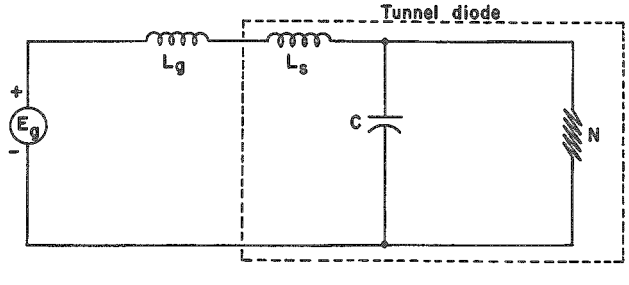

Fig. 1.0-4
CLN circuit: two reactive elements.

The most interesting case includes all of the tunnel diode parameters and uses an external generator with an inductive impedance, as in Fig. 1.0-5. This circuit is analyzed by means of a modification of the Lienard method (see Section 2.3) which allows us to include R_g, and by singular point analysis (see Section 3).

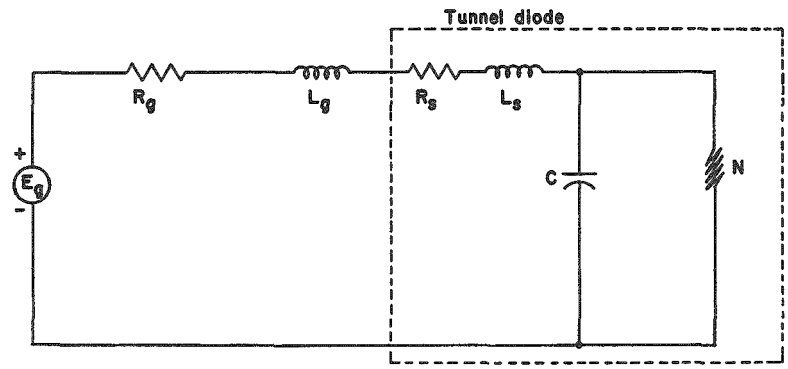

Fig. 1.0-5
RCLN circuit.

In any of these cases, I_g and E_g may be dc generators, as when the circuit is used as an oscillator, or they may be dc bias generators in series with pulse or ac generators, as when the circuit is used as a binary or as an amplifier.

Any change in E_g or I_g will cause a change in the steady-state operation of the circuit. For example, the diode may switch from one stable operating point to another, or the wave form produced by an oscillating circuit may change. The following analyses are readily applicable to these transitions.

2.1.1 Solution of a Simple RCN Circuit[1]

In some cases, relatively simple solutions of a simple RCN circuit are possible. For example, consider the circuit of Fig. 2.1.1-1, where $i_r = f(e_r)$ as given in Fig. 2.1.1-2. We have

$$I = \frac{e_r}{R} + C\frac{de_r}{dt} + f(e_r) \quad .$$

If the substitution $t = C\tau$ is made, this equation becomes,

$$\frac{de_r}{d\tau} = I - \frac{e_r}{R} - f(e_r) \quad .$$

Thus, we can obtain $de_r/d\tau$ as a function of e_r (see Fig. 2.1.1-3) by means of a graphical subtraction (see Fig. 2.1.1-2). This curve may be integrated graphically to yield e_r as a function of τ, the normalized time used to make $de/d\tau$ have units of current. A change of scale then yields e_r as a function of t.

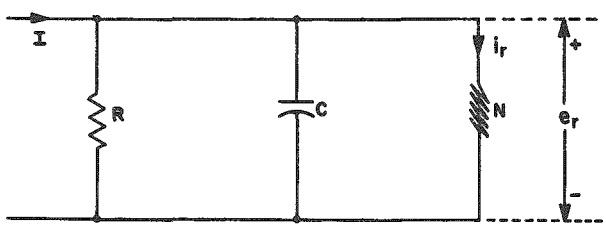

Fig. 2.1.1-1

RCN circuit

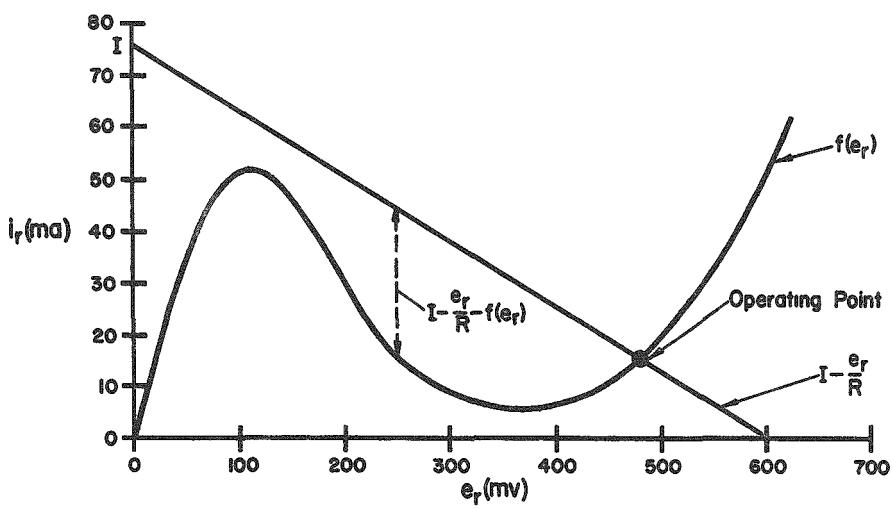

Fig. 2.1.1-2

Tunnel diode characteristic and load line.

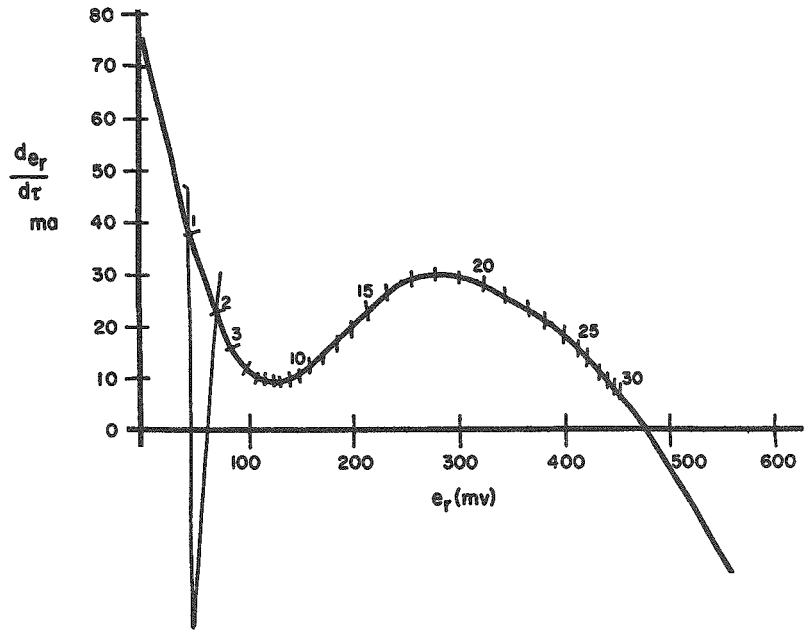

Fig. 2.1.1-3

The curve relates e_r to its time derivative. The graphical integration is performed by marking known time intervals on the curve.

In order to perform the graphical integration, we must mark off known $\Delta\tau$ intervals on the solution curve. The following derivation shows a simple way to do this (see Fig. 2.1.1-4). If $y \equiv de_r/d\tau$, then

$$\frac{\Delta e_r}{\Delta\tau} = y_{avg} = y_1 + \frac{\Delta y}{2} \quad ,$$

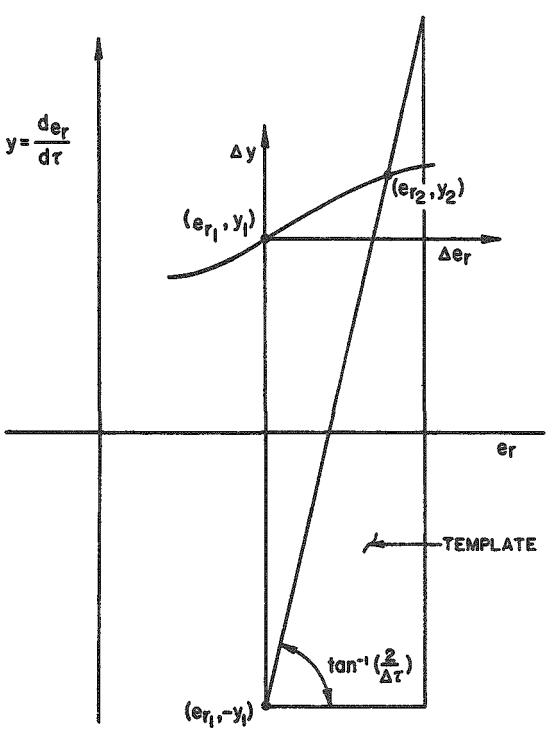

Fig. 2.1.1-4

Method for finding known time intervals.

from which we obtain

$$\Delta y = (2/\Delta\tau)\,\Delta e_r - 2y_1 \quad .$$

This is the equation of a straight line in the $(\Delta y, \Delta x)$ coordinate system. The point at which this line intersects the solution curve satisfies both the equation of the line and the solution of the circuit equation, and so the point (e_{r_2}, y_2) is reached $\Delta\tau$ after (e_{r_1}, y_1). Repetition of this process with suitable $\Delta\tau$'s will enable us to plot the final solution curve (see Fig. 2.1.1-5).

It may be helpful in some cases to vary $\Delta\tau$ in order to keep the points a convenient distance apart. For example, we chose I = 75 ma, R = 8 ohms,

N as in tunnel diode type 1N3130, and $\Delta\tau = 0.86$ ohm. For initial conditions $e_r = 0$ and $\tau = 0$, we obtain an increasing voltage which approaches the operating point asymptotically. If the initial voltage is chosen greater than the operating point voltage, we obtain a decreasing voltage which approaches the operating point voltage. Thus, we see that the operating point is stable.

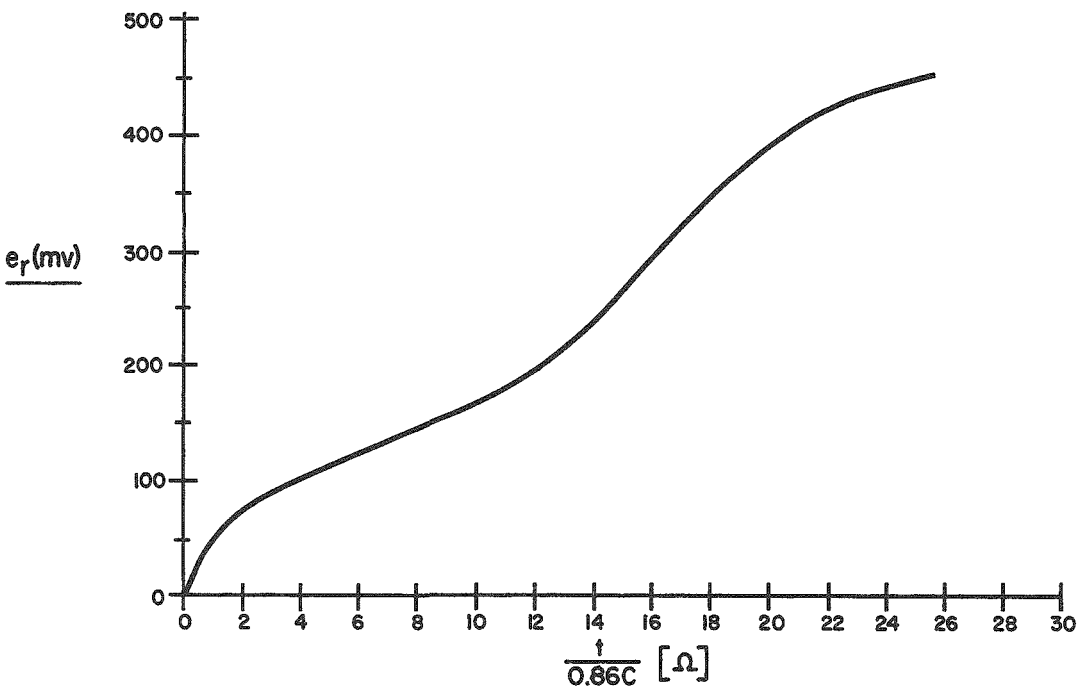

Fig. 2.1.1-5

Solution of the RCN circuit when I = 75 ma, R = 8 ohms, and N = 1N3130. The initial condition is $e_r = 0$ for t = 0.

2.1.2 RCN Case, Linear Approximation Method[1]

The circuit equations are (see Fig. 2.1.1-1)

$$C\frac{de_r}{dt} + i_r = I - \frac{e_r}{R} \text{ and } i_r = f(e_r) \quad .$$

The system is in equilibrium at the singular point (e_s, i_s) that satisfies simultaneously

$$i_s = I - \frac{e_s}{R} \text{ and } i_s = f(e_s), \text{ making } \frac{de_r}{dt} = 0 \quad .$$

Graphically, the singular point is the intersection of the load line with the tunnel diode characteristic (see Fig. 2.1.2-1).

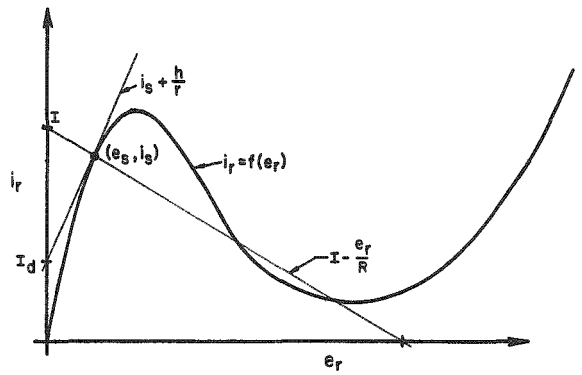

Fig. 2.1.2-1

Linear approximation to the tunnel diode characteristic around the operating point (or singular point).

Change of the variable e_r to $e_s + h$ yields

$$C\frac{dh}{dt} + f(e_s + h) = I - \frac{e_s}{R} - \frac{h}{R} \quad .$$

If only the linear terms of the power series of $f(e_r)$ around e_s are kept, there is obtained

$$f(e_s + h) \cong i_s + (h/r) \quad .$$

Then we finally obtain

$$C\frac{dh}{dt} = -h\left[\frac{1}{R} + \frac{1}{r}\right] \quad ,$$

where r is the tunnel diode resistance at (e_s, i_s).

Defining

$$\frac{1}{R_t} = \frac{1}{R} + \frac{1}{r} \text{ and } T = R_t C \quad ,$$

we obtain the first-order linear differential equation:

$$T\frac{dh}{dt} + h = 0 \quad .$$

The solution is

$$h = h_0 \exp\left(-\frac{t - t_0}{T}\right) \quad .$$

The definition $e_0 = e_r(t_0) = e_s + h_0$ leads to

$$e_r - e_s = (e_0 - e_s) \exp\left(-\frac{t - t_0}{T}\right) \quad .$$

Taking the natural logarithm,

$$\frac{t - t_0}{T} = \ln \frac{e_0 - e_s}{e_r - e_s} \quad .$$

Thus, if $T > 0$, then e_r approaches e_s as t increases; if $T < 0$, then $|e - e_s|$ increases.

Let us approximate the tunnel diode characteristic by a number of straight lines. For this example, we shall use four lines, as in Fig. 2.1.2-2, choosing R = 400 ohms, I = 1.325 ma, r_1 = diode resistance in region I = 50 ohms, r_2 = 160 ohms, $r_3 = \infty$, and r_4 = 50 ohms. Determination of the singular points yields e_{s1} = 50.1 mv, e_{s2} = -3.72 mv, e_{s3} = 490 mv, and e_{s4} = 458 mv. All except e_{s4} are virtual singularities, that is, they occur outside the region for which the corresponding straight line is a good approximation to the tunnel diode characteristic. However, the circuit acts as though the singularity were real, as long as it is operating in the corresponding region. Thus, in region I we have

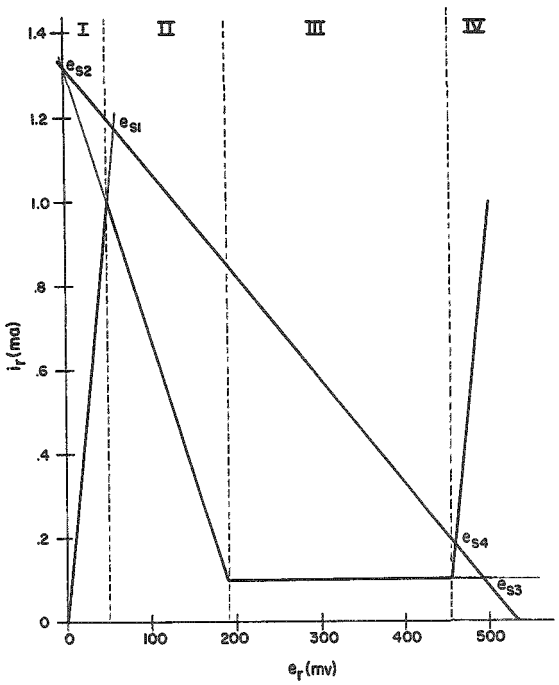

Fig. 2.1.2-2

Straight-line approximation to the tunnel diode characteristic.

$$\frac{e_r - 59.1}{e_0 - 59.1} = \exp \frac{(-t)}{R_t C} \quad ;$$

$$R_t = \frac{Rr}{R + r} = \frac{(400)(50)}{400 + 50} =$$

44.4 ohms;

this expression is valid as along as $e_r < 50$, the upper limit of region I. Choosing as initial conditions $e_r = 0$ and $t = 0$, we can calculate the time t/C it takes to go from $e_0 = 0$ to $e_f = 50$ mv:

$$\frac{t}{C} = R_t \ln \frac{e_0 - e_s}{e_f - e_s} = 44.4 \ln \frac{59.1 - 0}{59.1 - 50} = 83 \text{ ohms} \quad .$$

Calculations for the four regions yields the table

Region:	I	II	III	IV
Initial Value e_0 (mv)	0	50	194	455
Final Value e_f (mv)	50	194	455	458
Singular point e_s (mv)	59.1	- 3.72	490	458
Total Resistance R_t (ohm)	44.4	-266	400	44.4
Time per Region t/C (ohm)	83	339	855	∞

We can now graph our results as in Fig. 2.1.2-3. Of course, for a more accurate solution, one could use more straight lines to fit the diode characteristic better.

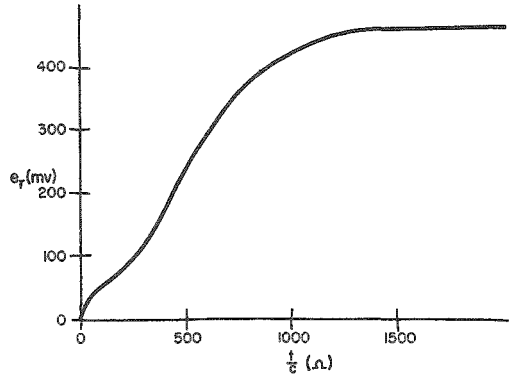

Fig. 2.1.2-3

Solution curve for the case shown in Fig. 2.1.2-2.

2.2.0 Isocline Method[1,2]

The three methods we describe in this and following sections deal with ways of finding the solution to the system of two first-order equations:

$$\frac{dx}{d\tau} = P(x, y) \quad ; \quad \frac{dy}{d\tau} = Q(x, y) \quad .$$

Later, we shall see that variables x and y are linearly related to a certain current and a certain voltage in the circuit under analysis. Variable τ is a normalized time.

We want to find the parametric solutions for the system:

$$x = x(\tau) \quad \text{and} \quad y = y(\tau) \quad .$$

If one differential equation is divided by the other, there is obtained a first-order differential equation:

$$\frac{dy}{dx} = \frac{Q(x, y)}{P(x, y)} \quad ,$$

from which time has been eliminated. The solution to this equation is a curve in the (x,y) plane, usually called the phase plane of the system.

The solution curve has a slope $s = dy/dx$ for each point of the phase plane, which can be calculated from

$$s = Q(x, y)/P(x, y) \quad .$$

Each point of the phase plane corresponds to a certain instantaneous energy distribution in the system. This means that we need to know the initial conditions, namely, x_0 and y_0 for $\tau = 0$. Drawing a small straight segment with slope $s_0 = Q(x_0, y_0)/P(x_0, y_0)$ through point x_0, y_0, we find point x_1, y_1 as another instantaneous state of the system. By repeating this procedure, we obtain the solution curve corresponding to the initial conditions. The construction in general ends when the solution curve reaches a certain stable condition. It can be either a point of the plane or a closed curve called the limit cycle.

To simplify the drawing of the solution curve, a set of curves called isoclines is drawn in the phase plane. An isocline is the locus of all points on the phase plane where dy/dx has a given value s_i. Thus, $Q(x,y) = s_i P(x,y)$ is the isocline algebraic equation.

Once an isocline is plotted on the phase plane, small line segments are drawn all along it having the chosen slope s_i (see Fig. 2.2.1-3).

To illustrate these concepts, take a very simple differential equation:

$$\frac{d^2x}{d\tau^2} + x = 0$$

with the well-known solution

$$x = K \sin(\tau+\phi) \quad ,$$

where K and ϕ are constants. This equation can be split into a system of two first-order equations:

$$\frac{dx}{d\tau} = y \text{ (by definition) and } \frac{dy}{d\tau} = -x \quad .$$

Dividing one by the other,

$$\frac{dy}{dx} = -\frac{x}{y} \quad .$$

The phase-plane solution to this equation is a circle

$$x^2 + y^2 = K^2$$

as can be proven by integrating the equation analytically.

The parametric solutions are

$$y = K \cos(\tau+\phi) \quad ; \quad x = K \sin(\tau+\phi) \quad .$$

The isoclines $y = -sx$ are straight lines radiating from the origin and perpendicular to the solution curve.

Returning to the general case, once we have the solution curve in the phase plane, the next step is to find the parametric solution $x = x(\tau)$. This can be done by plotting the derivative $dx/d\tau = P(x,y)$ with respect to x.

The graphical integration explained in Section 2.1.1 is then used to obtain $x = x(\tau)$. The same procedure yields $y = y(\tau)$.

2.2.1 LCN Case

The circuit to be solved is shown in Fig. 2.2.1-1. The method used here can also be used to solve the RLCN case (see Section 2.3.1).

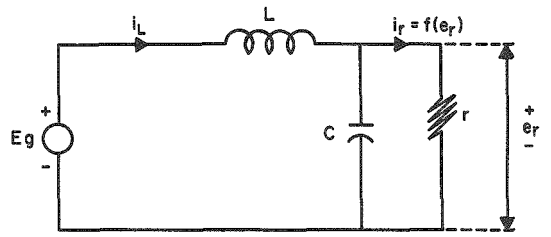

Fig. 2.2.1-1
LCN circuit.

The circuit equations are

$$L \frac{di_L}{dt} = E_g - e_r \qquad \text{loop equation} \quad ;$$

$$C \frac{de_r}{dt} = i_L - i_r \qquad \text{nodal equation} \quad ;$$

$$i_r = f(e_r) \qquad \text{tunnel diode characteristic} \quad .$$

It is convenient to normalize the time variable by defining $t = \sqrt{LC}\,\tau$. The new variable τ is a-dimensional because $\sqrt{LC}$ is the natural period of oscillation of the LC circuit. The substitution yields

$$\sqrt{\frac{L}{C}} \frac{di_L}{d\tau} = E_g - e_r$$

and

$$\sqrt{\frac{C}{L}} \frac{de_r}{d\tau} = i_L - i_r \quad .$$

Since $\sqrt{C/L}$ has the dimensions of an impedance, we can also define

$$I = \sqrt{C/L}\; E_g \quad \text{and} \quad i = \sqrt{C/L}\; e_r \quad .$$

These substitutions yield

$$\frac{di_L}{d\tau} = I - i \quad \text{and} \quad \frac{di}{d\tau} = i_L - i_r \quad ,$$

which have the same form as the ones studied in the preceding section. We can simplify them further by changing the coordinates. The new origin is taken on the characteristic curve at $i = I$. We shall see in Section 3.0 that this point of the phase plane is singular.

We define then:

$$i = I + y \quad ; \quad i_L = I_L + x \quad ,$$

where the constant I_L comes from $I_L = f(E_g)$. We also define the new function

$$\phi(y) = f(e_r) - I_L \quad ,$$

where

$$e_r = E_g + \sqrt{L/C}\, y$$

(see Fig. 2.2.1-2). Finally,

$$\frac{dx}{d\tau} = -y \quad ; \quad \frac{dy}{d\tau} = x - \phi(y) \quad .$$

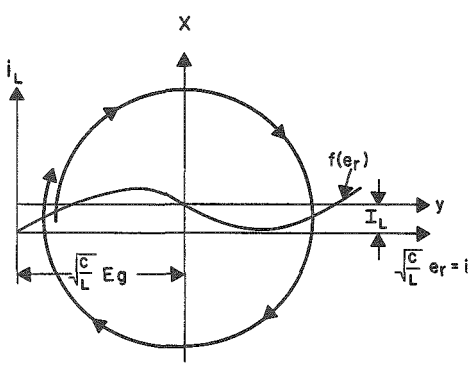

Fig. 2.2.1-2

Phase plane of the LCN circuit. The solution curve tends toward a nearly circular limit cycle when the value of $\sqrt{C/L}$ is large.

The first equation shows that x increases with time for points in the phase plane where $y < 0$ and decreases when $y > 0$ (see Fig. 2.2.1-2). Dividing one by the other,

$$\frac{dy}{dx} = -\frac{x - \phi(y)}{y} \quad .$$

A general idea of the meaning of this formula is obtained if we approximate $\phi(y)$ around the origin by a straight line:

$$\phi(y) \cong by$$

where

$$b = \sqrt{\frac{L}{C}}\, \frac{df(e_r)}{de_r}\,\Big|_{e_r = E_g} \quad ;$$

then

$$\frac{dy}{dx} = -\frac{x}{y} + b \quad .$$

If $|b| << 1$, then the equation becomes $dy/dx = -x/y$, whose solution, as already shown, is a circle corresponding to a sinusoidal oscillator. Because b is not really zero, the solution in the (x,y) plane moves with increasing amplitude ($b<0$) on a spiral around the origin. This spiral tends to a limit cycle when the solution curve reaches regions over which $d\phi(y)/dy > 0$. As an example, we solve a circuit with the following values (see Fig. 2.2.1-1):

$L = 1.2$ nhy ; $C = 12$ pfd ; $E_g = 200$ mv ;

N : 1N3130 characteristic.

The normalizing factors are:

$$\sqrt{L/C} = 10 \text{ ohms} \quad \text{and} \quad \sqrt{LC} = 120 \text{ p sec.}$$

Fig. 2.2.1-3 shows the isoclines plotted with $x = F(y) - sy$, with

$$s = \frac{dy}{dx} = -2, -1, 0 \text{ and } +1 \quad .$$

The initial conditions are arbitrarily chosen as $t = 0$, $e_r = 158$ mv, and $i_L = 35$ ma. The solution curve is easily traced starting at this point.

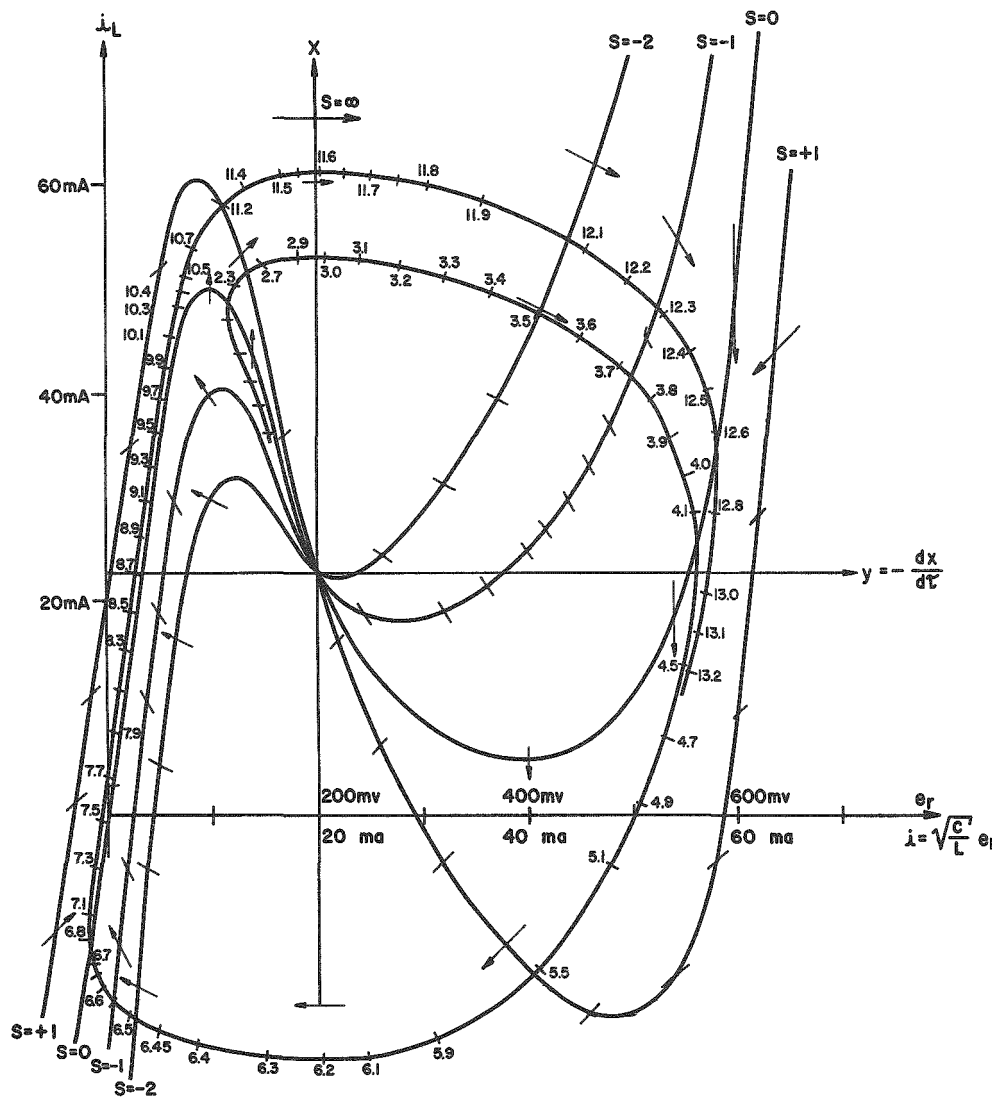

Fig. 2.2.1-3

Isoclines and solution curve. The initial conditions are: $t = 0$, $e_r = 158$ mv, and $i_L = 35$ ma.

In this example, the solution rapidly reaches the limit cycle. This limit cycle does not depend on the initial conditions and represents the steady-state operation of the oscillatory circuit.

Similarly to Section 2.1.1, we have a curve relating x to its derivative y. We can then use the same graphical method of integration to obtain $e_r = e_r(t)$. To obtain the solution curve shown in Fig. 2.2.1-4, we have used, instead, the method of Section 2.3.0.

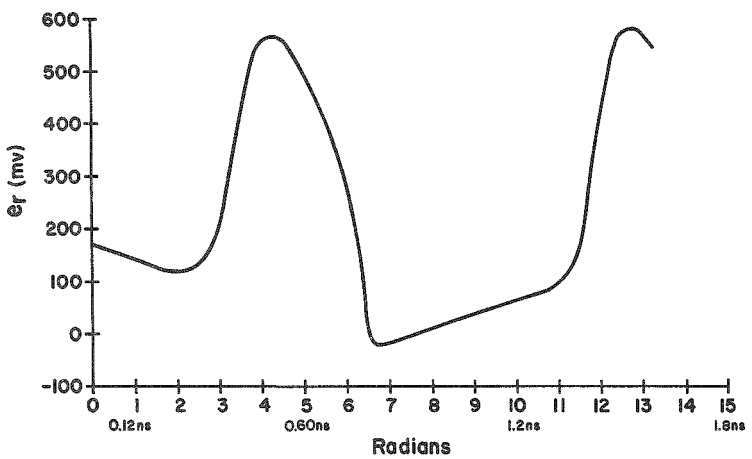

Fig. 2.2.1-4
Solution curve.

2.3.0 Modified Lienard Method

The chief disadvantage of the isocline method is that plotting the isoclines entails considerable effort. This would not be too serious a disadvantage if the same isoclines were to be used for a number of different initial conditions, but this is frequently not the case. The modified Lienard method avoids the tedious plotting of isoclines, but has the disadvantage that the construction must be repeated for each set of initial conditions.

The Lienard method that solves the equation

$$\frac{dz}{dx} = \frac{\phi(z) - x}{z}$$

for $z = z(x)$ has been modified in a way that makes it suitable for solving the more general differential equation

$$\frac{dz}{dx} = \frac{\phi[z + F(x)] - x - z\,\frac{d}{dx}[F(x)]}{z} \quad ,$$

where F and ϕ are arbitrary single-valued functions.

As in the preceding section, there is a second equation relating the two variables x and z to a normalized time τ:

$$\frac{dx}{d\tau} = -z \quad .$$

It is convenient to define a new variable $y = z + F(x)$; substituting z by $y - F(x)$, we obtain:

$$\frac{dy}{dx} - \frac{dF(x)}{dx} = \frac{\phi(y) - x}{y - F(x)} - \frac{dF(x)}{dx} \quad ,$$

and, simplifying,

$$\frac{dy}{dx} = \frac{\phi(y) - x}{y - F(x)} \quad ; \quad \frac{dx}{d\tau} = F(x) - y \quad .$$

The first of these equations solved by using the graphical construction is shown in Fig. 2.3.0-1. Representing x on the vertical axis and y on the horizontal axis, we can plot $\phi(y)$ and F(x) as shown. Choosing a point P_0 corresponding to the initial conditions, the construction begins by drawing a line through P_0 parallel to the x-axis until it intersects the $\phi(y)$ curve at Q, and a line through P_0 parallel to the y-axis until it intersects the F(x) curve at S. Then, complete the defined rectangle P_0QRS and draw the diagonal RP_0. Now draw a line segment through P_0 perpendicular to RP_0. This segment is tangent to the solution curve at P_0. We then choose a new point P_1, Δs from P_0 and on the tangent segment, and repeat the construction.

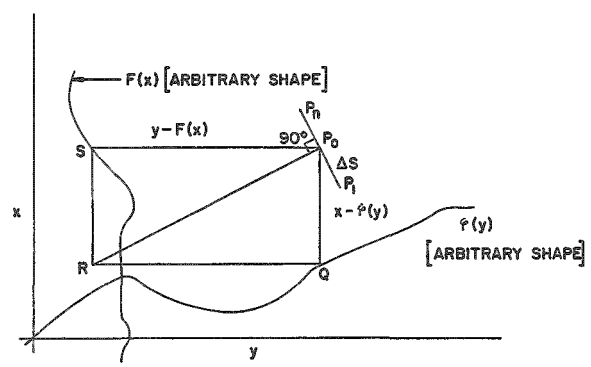

Fig. 2.3.0-1
Modified Lienard graphical construction.

To verify the construction, we note that angle RP_0Q = angle SP_0P_n. Then $\tan \angle RP_0Q = \tan \angle SP_0P_n$, $\tan \angle RP_0Q = -\frac{F(x) - y}{x - \phi(y)}$ by construction, and any curve that goes through point P_0 and is tangent to segment P_nP_1 has a derivative

$$\frac{dy}{dx} = -\tan \angle SP_0P_n \quad .$$

To find y as a function of τ, we may mark off known $\Delta\tau$ intervals on the solution curve and integrate graphically. A method for marking known $\Delta\tau$ intervals during the construction follows.

Figure 2.3.0-2 shows that triangle RQP_0 is similar to triangle P_0AP_1; then,

$$\frac{\Delta s}{\rho} = \frac{\Delta x}{F(x) - y} \quad ,$$

and also

$$\tan \Delta\omega = \frac{\Delta s}{\rho}$$

or

$$\Delta\omega = \frac{\Delta s}{\rho}$$

if $\Delta\omega$ is a small angle measured in radians. Therefore,

$$\Delta\omega = \frac{\Delta x}{F(x) - y} \quad ,$$

and since

$$\frac{dx}{d\tau} = F(x) - y \quad ,$$

we conclude that

$$\Delta\omega = \Delta\tau \quad .$$

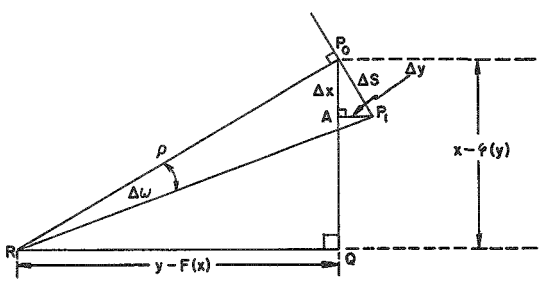

Fig. 2.3.0-2

Method for marking known time intervals on the solution curve.

Thus, if we choose Δs in each construction so that $\Delta\omega$ is known, we will have known $\Delta\tau$ intervals between P_0 and P_1. For performing the construction, it is convenient to have a template for each value of $\Delta\omega$ that is used.

2.3.1 RLCN Case

We now give a physical meaning to the theory of the preceding section. Consider the circuit of Fig. 2.3.1-1. We have

$$L\frac{di_L}{dt} = E - Ri_L - e_r \quad ;$$

$$C\frac{de_r}{dt} = i_L - i_r \quad ,$$

where

$$i_r = f(e_r) \quad .$$

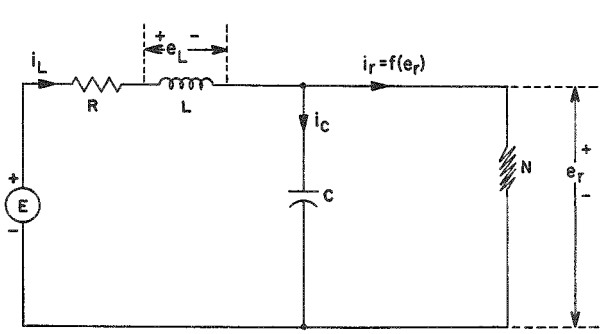

Fig. 2.3.1-1

RCLN circuit.

As in Section 2.2.1, we normalize time and voltages by defining

$$t = \sqrt{LC}\,\tau \quad ; \quad \sqrt{C/L}\,R = K \quad ;$$

$$\sqrt{C/L}\,E = I \quad ; \quad \sqrt{C/L}\,e_r = i \quad .$$

Substitution in the above equations yields

$$\frac{di_L}{d\tau} = I - Ki_L - i$$

and

$$\frac{di}{d\tau} = i_L - i_r = i_L - \phi(i) \quad ,$$

where

$$\phi(i) = f(e_r) = i_r \quad .$$

Dividing one by the other gives

$$\frac{di_L}{di} = \frac{I - Ki_L - i}{i_L - \phi(i)} \quad ,$$

an equation of the form treated in Section 2.3.0, with:

$$i_L = x \quad ; \quad i = y \quad ; \quad F(x) = I - Ki_L \quad ; \quad \phi(y) = \phi(i) \quad .$$

This equation can be solved by the same construction, as shown in Fig. 2.3.1-2. The equation has also the form $dy/dx = Q(x,y)/P(x,y)$ already seen in Section 2.2.0 and can thus be solved by the isocline method.

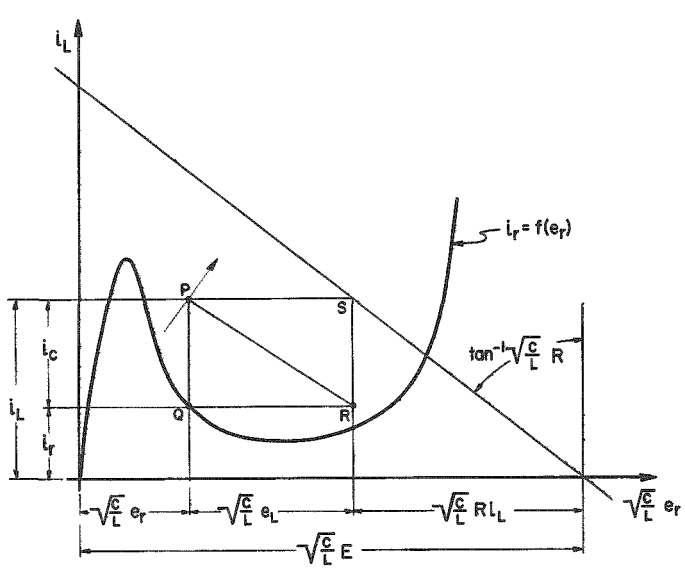

Fig. 2.3.1-2

The modified Lienard method in the case of the RLCN circuit. The *same* scale must be used for both axes. The relationships between voltages and currents are shown.

To find Δt from $\Delta\omega$, we have

$$\Delta\omega = \Delta\tau = \Delta t/\sqrt{LC} \quad .$$

Then

$$\Delta t = \sqrt{LC}\,\Delta\omega \quad .$$

It is important to note that this method, unlike the isocline method, requires the use of the same scale, in amperes, on both axes. The equation

$$\frac{di}{d\tau} = i_L - \phi(i)$$

shows that i increases for all points of the phase plane where $i_L > \phi(i)$ and decreases for $i_L > \phi(i)$.

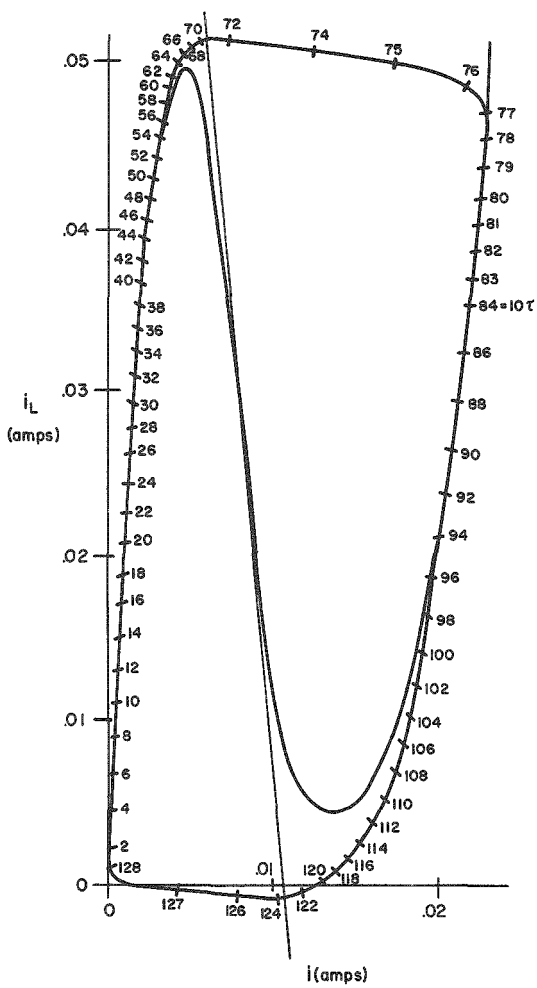

Fig. 2.3.1-3

Phase plane solution curve obtained by applying the modified Lienard method. The initial point ($i = i_L = 0$ for $t = 0$) is very near the limit cycle.

Example 1.

Solve a RLCN circuit with L = 10 nhy, C = 20 pfd, R = 2.0 ohm N as in tunnel diode type 1N3130, E = 240 m volts; (see Fig. 2.3.1-3)

$$\sqrt{\frac{C}{L}} = 0.0447 \text{ mhos}$$

and

$$\sqrt{LC} = 44.7 \text{ p sec/radian} \quad .$$

Choosing initial conditions $i = i_L = 0$ and performing the construction with $\Delta\omega = 0.1$ or 0.2 radians as convenient, the solution is the curve shown in Fig. 2.3.1-3. The numbers along the curve are the cumulative number of tenths of radians. Knowing that $t = \sqrt{LC}\,\omega$ and that $e_r = \sqrt{\frac{L}{C}}\,i$ the wave shape shown in Fig. 2.3.1-4 is obtained.

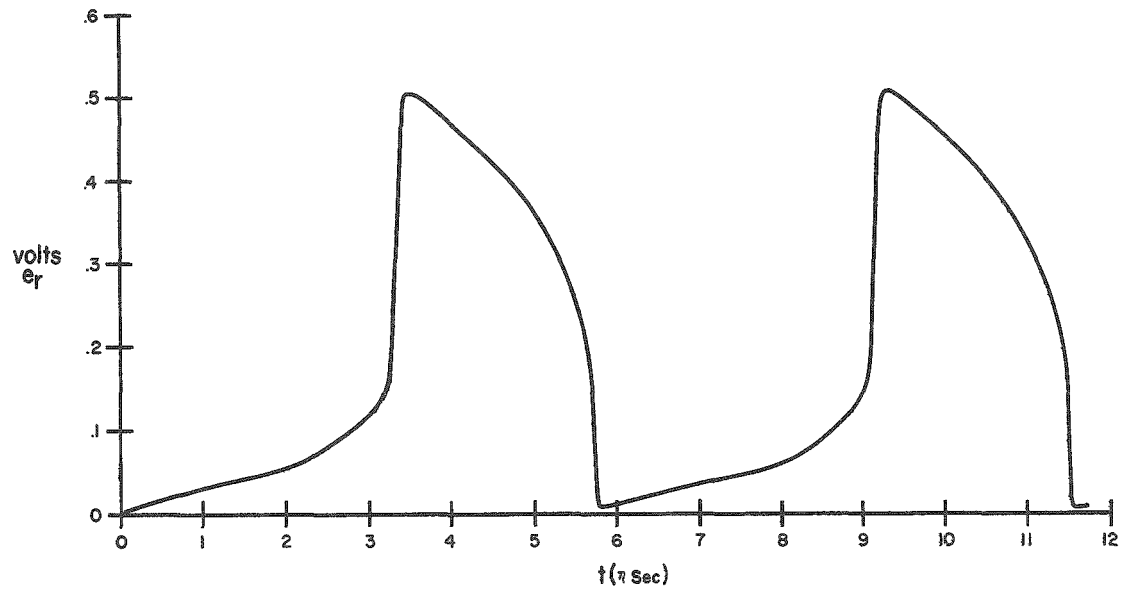

Fig. 2.3.1-4

Wave form produced by a RCLN circuit when R = 2 ohms, L = 10 nhy, C = 20 pfd, N = 1N3130, E = 240 mv. The circuit is a relaxation oscillator.

Example 2.

The circuit to be solved is again a RLCN. The parameters are

L = 1.2 nhy ; C = 12 pfd ; R = 13.3 ohms ;

N = 1N3130 characteristic .

This circuit is the same LCN used as an example in Section 2.2.1, except that it has a resistance R in series with the generator.

The generator is a combination of a bias voltage E_1 in series with a pulse generator $e_2 = E_2 [u(t) - u(t - T)]$, where E_2 is a constant and u is a step function (see Fig. 2.3.1-5).

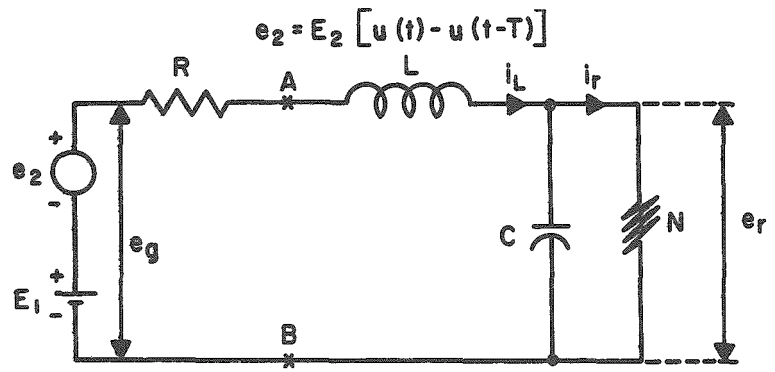

Fig. 2.3.1-5
Flip-flop circuit.

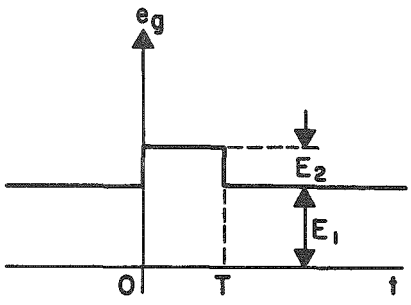

Fig. 2.3.1-6

Total voltage $e_g(t)$.

The total voltage e_g is a function of time as shown in Fig. 2.3.1-6. If we choose E_1 = 700 mv, we see that the load line for R = 13.3 ohms cuts the characteristic curve (see Fig. 2.3.1-7) in three points: L, M, and O. We prove in the next section that points L and O_1 are stable operating points of the circuit and that M is unstable. We have then a flip-flop. If the circuit is at point L for negative times when a positive pulse e_2 of 200 mv is applied at t = 0, the load line is shifted as shown in Fig. 2.3.1-7. The new load line only intersects the characteristic curve at one point, O_2. Being this point stable, the system is triggered to singular point O_2. The solution curve goes from L to O_2 as shown in Fig. 2.3.1-7 if T is infinite.

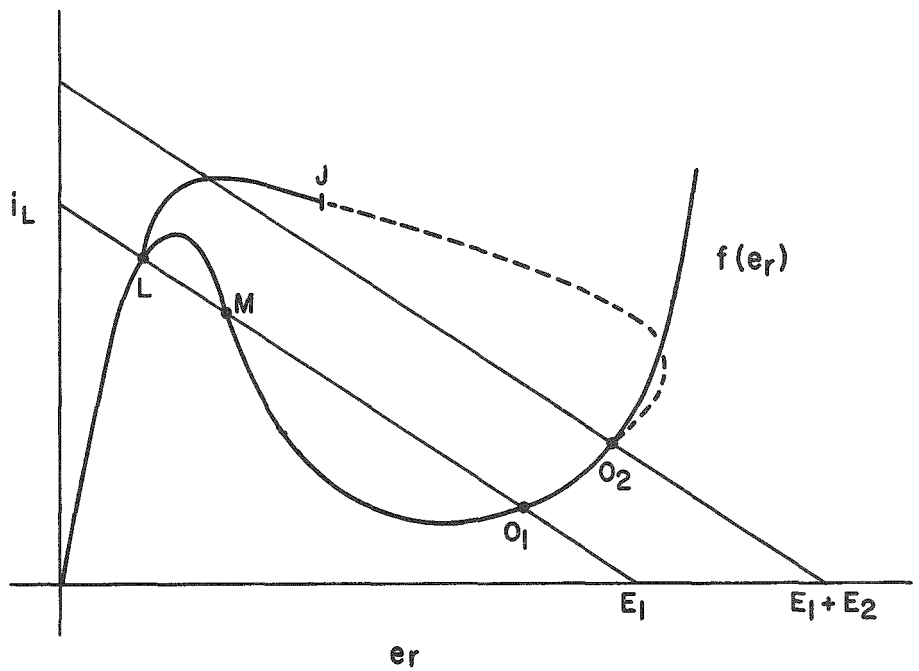

Fig. 2.3.1-7

Bistable RCLN phase plane. The phase-plane solution is always a continuous curve because neither the current through an inductor (i_L) nor the voltage across a capacitor (e_r) can be discontinuous.

If the pulse duration is finite, then, when the solution curve has reached a certain point J, the load line returns to its original position and the system has again two stable points, L and O_1. There is a certain point J of no return. If the trigger pulse disappears before this point is reached, the system goes back to point L.

The solution curve from time T to infinity starts at point J and is graphically computed by use of the load line O_1ML.

The actual construction for the parameters we give above is shown in Fig. 2.3.1-8. The solution curve splits in two branches at point J. Solution curve number 1 corresponds to the case $T \to \infty$, and number 2 to the case $T = 1.9\sqrt{LC} = 1.9 \times 0.120$ nsec.

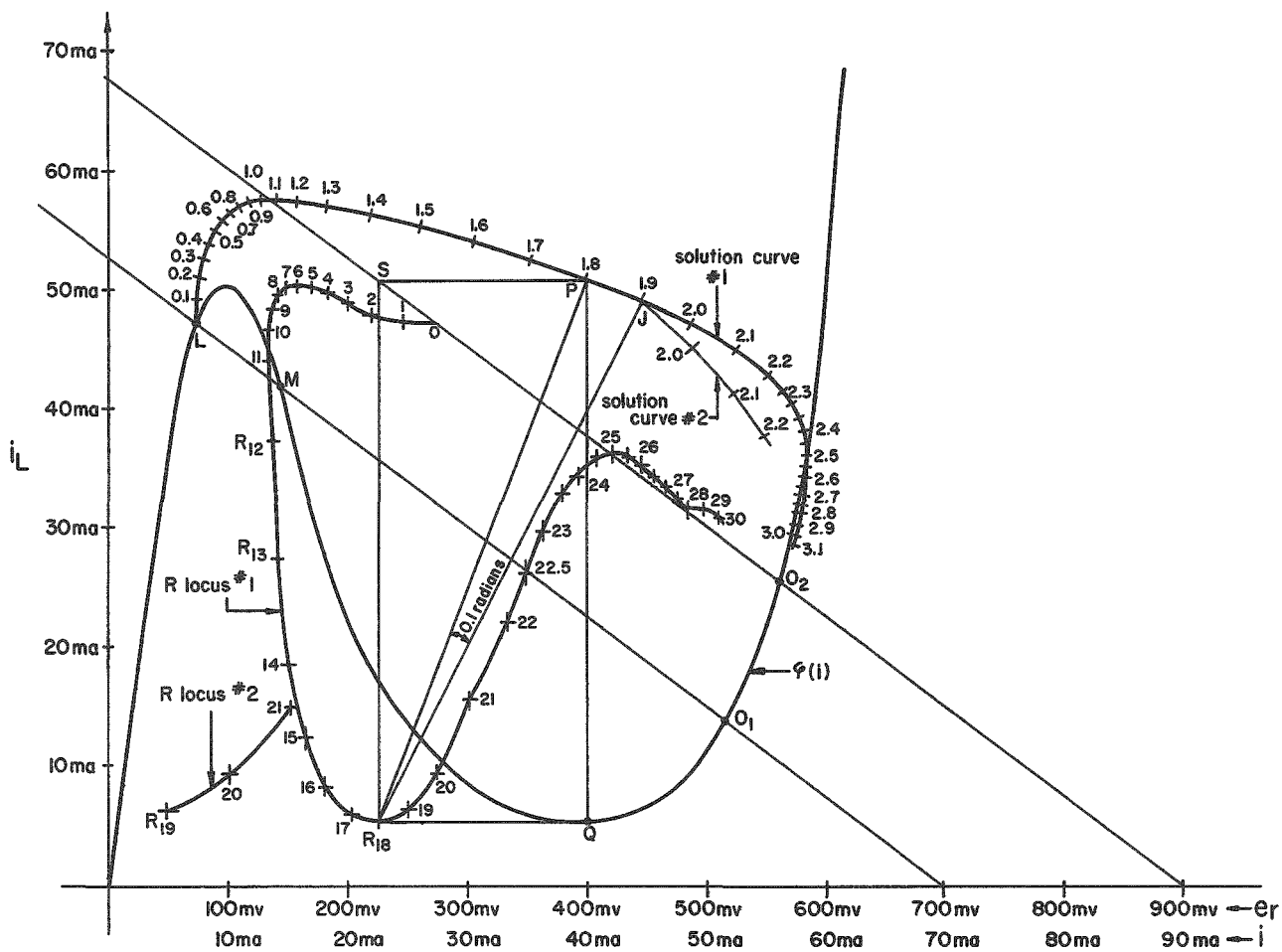

Fig. 2.3.1-8

Phase-plane solution curve obtained by the modified Lienard method. The parameters are $E_1 = 700$ v, $E_2 = 200$ v, R = 13.3 ohms, L = 1.2 nhy, C = 12 pfd, and N = 1N3130.

The locus of the R points is also shown for both cases. It may be used during the construction of the solutions to evaluate the accuracy of the approximations. While this construction is performed, it is possible to evaluate qualitatively how near we are to the exact solution. When successive R points get too far apart, it is convenient to choose a template with smaller angles.

We can now plot the voltage across the tunnel diode against time. In the circuit of Fig. 2.3.1-5 this voltage appears between points A and B:

$$e_{AB} = e_r + e_L$$

(see Fig. 2.3.1-2). This curve is shown in Fig. 2.3.1-9.

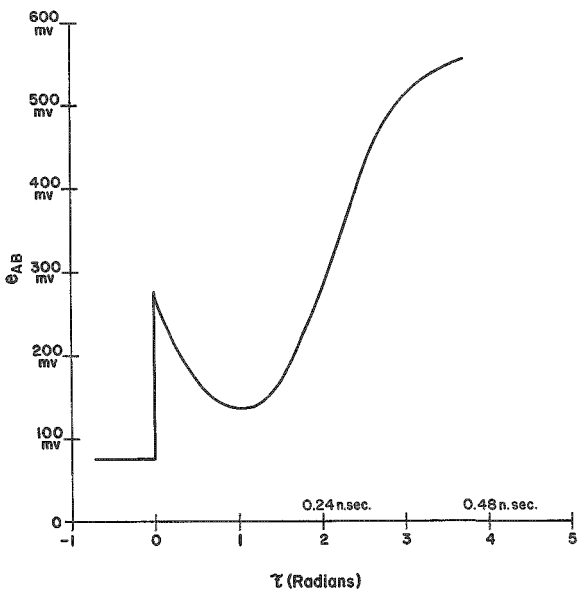

Fig. 2.3.1-9

Switching transient of the bistable RCLN circuit.

3.0 Analysis of Singular Points[1,2]

This method is a combined analytical and graphical approach. The method consists of:

a) location of the differential equation singularities;

b) determination by analytical methods of the solution curves around the singularities. This is usually simple, because the first two (linear) terms of a Taylor series can be used as an approximation to the nonlinear functions in the vicinity of the singularities;

c) approximate determination of the solution by observing the location of the singularities and the nature of the solution curves near them.

We wish to solve the system:

$$\frac{dx}{d\tau} = P(x,y) \quad ; \quad \frac{dy}{d\tau} = Q(x,y) \quad .$$

Expanding in Taylor series about (x_s,y_s) and keeping only the linear terms, there is obtained

$$\frac{dx}{d\tau} = P(x_s,y_s) + (x - x_s)\, A + (y - y_s)\, B \quad ;$$

$$\frac{dy}{d\tau} = Q(x_s,y_s) + (x - x_s)\, C + (y - y_s)\, D \quad .$$

The point (x_s,y_s) is a singularity when $P(x_s,y_s) = Q(x_s,y_s) = 0$. Since the time derivatives $\dot{x}$ and $\dot{y}$ are zero at (x_s,y_s), we see that a singularity is a point of equilibrium.

If a change is made to co-ordinates

$$x = x_s + h_1 \quad ; \quad y = y_s + h_2$$

then,

$$\frac{dh_1}{d\tau} = h_1 A + h_2 B \quad ; \quad \frac{dh_2}{d\tau} = h_1 C + h_2 D \quad .$$

This is a linear system equivalent to the original one near the singularity.

The general solution is of the form:

$$h_1 = H_{11} \exp(\lambda_1 \tau) + H_{12} \exp(\lambda_2 \tau) \quad ;$$

$$h_2 = H_{21} \exp(\lambda_1 \tau) + H_{22} \exp(\lambda_2 \tau) \quad ,$$

where H_{11}, H_{12}, H_{21}, and H_{22} are constants determined from the initial conditions.

Constants λ_1 and λ_2 are calculated as follows. Write the differential equation in matrix form:

$$\begin{bmatrix} \dot{h}_1 \\ \dot{h}_2 \end{bmatrix} = \begin{bmatrix} A & B \\ C & D \end{bmatrix} \begin{bmatrix} h_1 \\ h_2 \end{bmatrix}$$

where

$$\dot{h}_1 = \frac{dh_1}{d\tau} \quad \text{and} \quad \dot{h}_2 = \frac{dh_2}{d\tau} \quad ,$$

or, in a more condensed form,

$$[\dot{h}] = [M]\,[h] \quad .$$

Assuming

$$h = H \exp(\lambda \tau)$$

as a solution, then

$$\lambda [h] = [M]\,[h] \quad ,$$

from which we obtain

$$\left[[M] - \lambda [I] \right] = [0] \quad ,$$

where $[I]$ is the unit matrix and $[0]$ is the null matrix. This matrix equation is satisfied if for its determinant

$$\begin{vmatrix} A - \lambda & B \\ C & D - \lambda \end{vmatrix} = 0$$

or

$$(A - \lambda)(B - \lambda) - BC = 0 \quad .$$

The roots of this quadratic equation are called the eigenvalues of matrix [M]:

$$\lambda_{1,2} = \frac{1}{2}\left\{(A + D) \pm \sqrt{(A + D)^2 + 4\,(BC - AD)}\right\}$$

$$= \frac{1}{2}\left\{A + D \pm \sqrt{(A + D)^2 + 4\,BC}\right\}$$

$$= \beta \pm \sqrt{\alpha} \quad .$$

We introduce now a linear transformation:

$$h_1 = P_{11}u_1 + P_{12}u_2 \quad ; \quad h_2 = P_{21}u_1 + P_{22}u_2 \quad ,$$

where the P's are constant. This transformation changes the (h_1, h_2) plane into the (u_1, u_2) plane (see Fig. 3.0-1) in such a way that a straight line is transformed into a straight line, but in general the angles are changed. In this form a rectangle is transformed into a parallelogram.

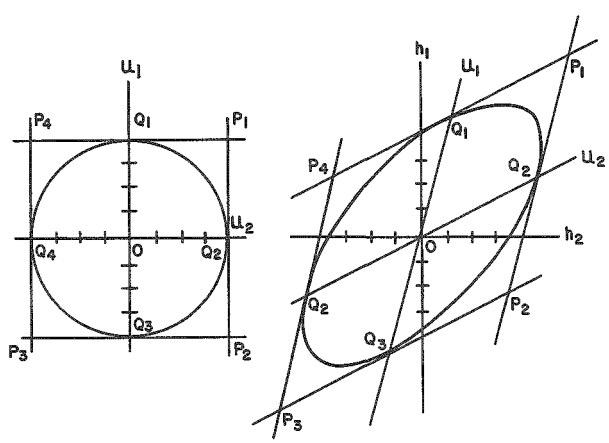

Fig. 3.0-1

Linear transformation between plane (h_1, h_2) and plane (u_1, u_2). Corresponding points and lines are indicated.

We can express the above transformation in matrix form:

$$[h] = [P]\,[u] \qquad \text{if } |P| \neq 0 \quad ,$$

and

$$[\dot{h}] = [P]\,[\dot{u}] \quad .$$

Substitution into the matrix equation yields

$$[P]\,[\dot{u}] = [M]\,[P]\,[u]$$

or

$$[\dot{u}] = [N]\,[u] \quad ,$$

where

$$[N] = [P]^{-1}\,[M][P] \quad .$$

Since [M] and [N] have the same eigenvalues, a suitable choice of [P] will serve to diagonalize N. This means that

$$[N] = \begin{bmatrix} \lambda_1 & 0 \\ 0 & \lambda_2 \end{bmatrix} \quad .$$

Then

$$\dot{u}_1 = \lambda_1 u_1 \quad ; \quad \dot{u}_2 = \lambda_2 u_2 \quad ,$$

and the parametric solutions are

$$u_1 = U_1 \exp(\lambda_1 \tau) \quad ; \quad u_2 = U_2 \exp(\lambda_2 \tau) \quad .$$

To clarify this point, suppose that λ_1 and λ_2 are positive real numbers. In this case, the solution curves on plane (u_1, u_2) may look like the ones shown in Fig. 3.0-2. In the same figure the corresponding solution curves are shown on the (h_1, h_2) plane. The figure corresponds to the case for which $0 < \lambda_1 < \lambda_2$ and shows how the curves start from the origin with the u_1 direction and gradually tend to the u_2 direction. It is important to notice that axes u_1 and u_2 belong to the solution curve family.

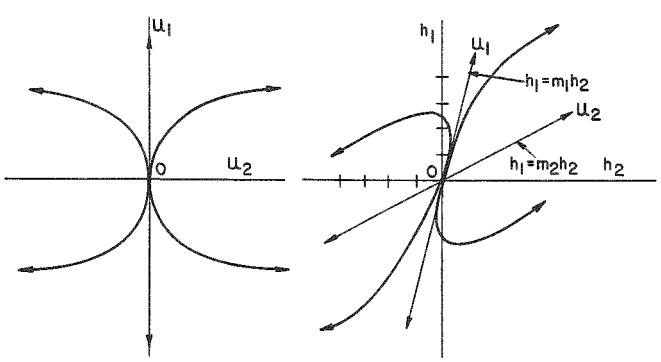

Fig. 3.0-2.

The same set of solution curves is shown in normal form (left) and in general form (right).

We can find the dirctions of the axes u_1 and u_2 in the plane (h_1, h_2) by using the isocline method. Dividing one differential equation by the other, there is obtained

$$\frac{dh_1}{dh_2} = \frac{Ah_1 + Bh_2}{Ch_1 + Dh_2} = s = \text{slope}.$$

Then

$$Ah_1 + Bh_2 = sCh_1 + sDh_2$$

and

$$h_1 = \frac{sD - B}{A - sC} h_2 = nh_2 \quad .$$

The isoclines are straight lines radiating from the singular point with slope

$$n = \frac{sD - B}{A - sC} \quad .$$

Axes u_1 and u_2 are solution curves for the problem; therefore, for them the slope of the solution curve and the slope of the isocline coincide. Let us call this particular slope

$$m = n = s \quad .$$

Then

$$m = \frac{mD - B}{A - mC}$$

or

$$m^2 + \frac{D - A}{C} m - \frac{B}{C} = 0 \quad .$$

The roots are

$$m_{1,2} = \frac{1}{2C} \left\{ A - D \pm \sqrt{(A - D)^2 + 4BC} \right\} = \gamma \pm \sqrt{\alpha} \quad .$$

Two other interesting isoclines are the ones corresponding to $s = 0$ and $s \to \infty$. If $s = 0$, then $n_0 = -B/A$. If $s \to \infty$, then $n_\infty = -D/C$.

It is also useful to know the slope of the solution curve for the axes h_1 and h_2. For

$$n \to \infty \ (h_1 \text{ axis}) \quad , \quad s_1 = A/C \, ,$$

and for

$$n = 0 \ (h_2 \text{ axis}) \quad , \quad s_2 = B/D \quad .$$

An example is shown in Fig. 3.0-3, where

$$A = -\frac{1}{2} \quad ; \quad B = -1 \quad ; \quad C = 1 \quad ; \quad D = -3 \quad .$$

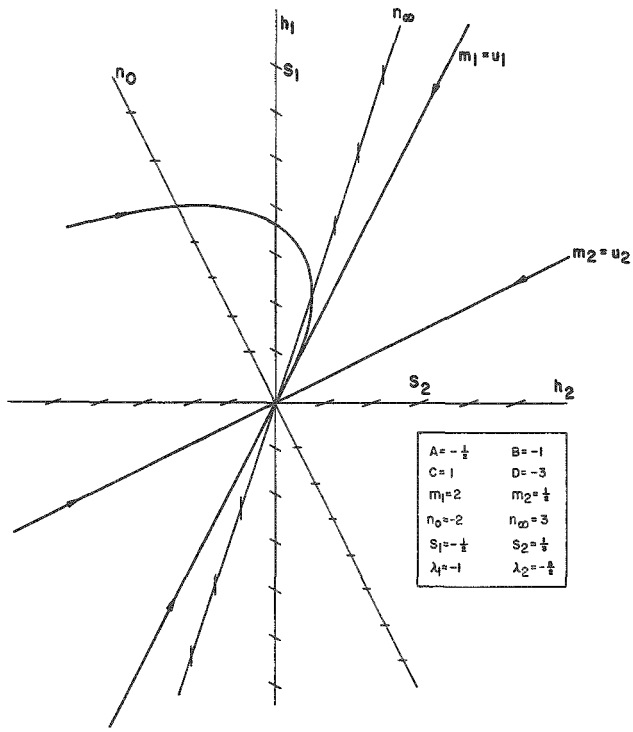

Fig. 3.0-3

The solution curve around the singularity can be found from an isocline construction.

If we always chose

$$\lambda_1 = \beta + \sqrt{\alpha} \quad ; \quad \lambda_2 = \beta - \sqrt{\alpha} \quad ;$$

$$m_1 = \gamma + \sqrt{\alpha} \quad ; \quad m_2 = \gamma - \sqrt{\alpha} \quad ,$$

then the final directions of the solution curves are parallel to m_1 for $t = +\infty$ and parallel to m_2 for $t = -\infty$.

Up to this point we have only considered the case $\alpha > 0$. If $\alpha < 0$, then λ_1, λ_2, m_1, and m_2 are complex numbers. Therefore, the solution curves do not have final directions. Instead, the curves will spiral around the singular point. The solution curve can be drawn using the isoclines n_0 and n_∞, and the slopes s_1 and s_2.

We can classify the singular point according to the nature of λ_1 and λ_2 as shown in the following table:

λ_1, λ_2	type of singularity
real, same sign	node
real, opposite sign	saddle point
pure imaginary	vortex
complex conjugates	focus

Singular points are points of stable or unstable equilibrium. A saddle point is always a point of unstable equilibrium. Nodes and foci are stable when $\beta < 0$ and unstable when $\beta > 0$.

This classification and conditions are shown in Fig. 3.0-4.

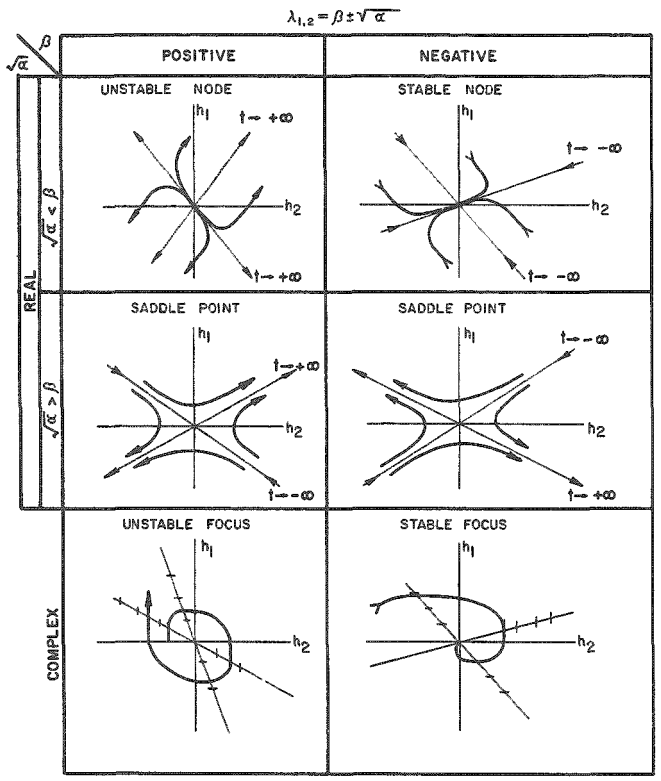

Fig. 3.0-4

Classification of singular points and typical solution curves.

3.1 RCLN Case

In Section 2.3.1 we found for the circuit shown in Fig. 2.3.1-1 the following normalized equations:

$$\frac{di_L}{d\tau} = I - Ki_L - i \quad ;$$

$$\frac{di}{d\tau} = i_L - \phi(i) \quad .$$

The singular points are determined by solving the system of equations:

$$I - Ki_L - i = 0 \quad ;$$

$$i_L - \phi(i) = 0 \quad .$$

The first one is a straight line and the second one is the tunnel diode characteristic. The characteristic curve is such that we have either one or three singular points. Calling the coordinates of the singular point i_S and i_{LS} and defining h_1 and h_2 by

$$i_L = i_{LS} + h_1 \quad ; \quad i = i_S + h_2 \quad ,$$

we obtain

$$\frac{dh_1}{d\tau} = I - Ki_{LS} - Kh_1 - i_S - h_2 \quad ;$$

$$\frac{dh_2}{d\tau} = i_{LS} + h_1 - \phi(i_S + h_2) \quad .$$

Expansion in a Taylor series around i_S gives

$$\phi(i_S + h_2) \cong \phi(i_S) + h_2\, \phi'(i_S) \quad .$$

Substitution and simplification yields

$$\frac{dh_1}{d\tau} = -Kh_1 - h_2 \quad ; \quad \frac{dh_2}{d\tau} = h_1 - \frac{1}{k} h_2 \quad .$$

If it is remembered that

$$\phi(i) = f(e_r) \quad ,$$

where

$$i = \sqrt{C/L}\, e_r \quad ,$$

then

$$\frac{d\phi(i)}{di} = \frac{df(e_r)}{de_r} \cdot \frac{de_r}{di} = \frac{1}{r}\sqrt{\frac{L}{C}} \quad .$$

Then

$$k = r\sqrt{C/L} \quad ,$$

where r stands for the tunnel diode resistance at the singular point (See Fig. 3.1-1).

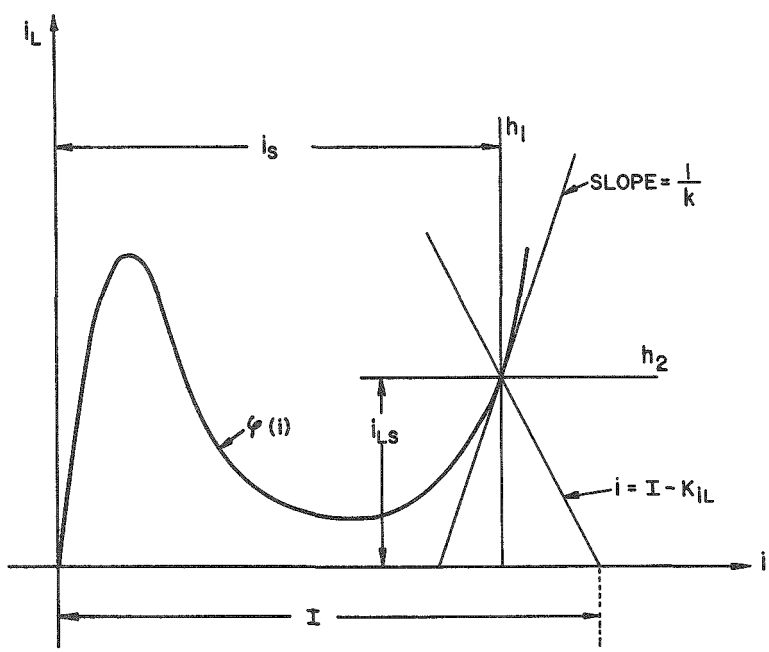

Fig. 3.1-1

Singular-point analysis of a RCLN circuit.

The matrix elements are: A = -K, B = -1, C = 1, D = -1/k.

By means of the formulas of Section 3.0, we find

$$\lambda_{1,2} = \frac{1}{2}\left\{-\left(K + \frac{1}{k}\right) \pm \sqrt{\left(K + \frac{1}{k}\right)^2 - 4\left(\frac{K}{k} + 1\right)}\right\} \quad ;$$

$$m_{1,2} = \frac{1}{2}\left\{\frac{1}{k} - K \pm \sqrt{\left(\frac{1}{k} - K\right)^2 - 4}\right\} \quad ;$$

$$n_0 = -1/K \quad ; \quad n_\infty = 1/k \quad ; \quad s_1 = -K \quad ; \quad s_2 = k \quad .$$

The singular point can be found graphically, as shown in Fig. 3.1-1. If the tangent to the characteristic curve be drawn, the value of k can be determined. Figure 3.0-3 is a construction based on the parameters obtained from Fig. 3.1-1, and the solution curve so obtained is accurate if the difference between $\phi(i)$ and $i_{Ls} + (h_2/k)$ is small.

3.1.1 Virtual Singular Points

Consider the situation, shown in Fig. 3.1.1-1, similar to the one described in the second example of Section 2.3.1. The circuit has only one stable state, located at s_2. Therefore, all solution curves end at that point.

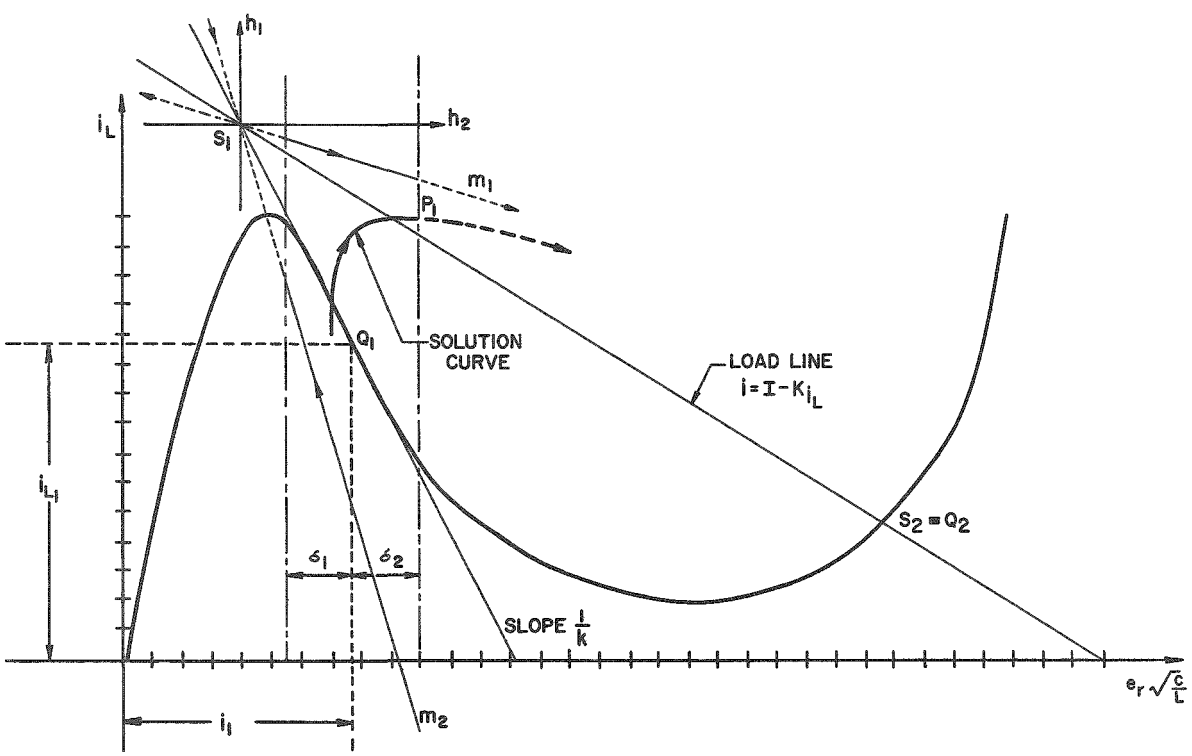

Fig. 3.1.1-1

Singular point analysis in the case of a virtual saddle point.

The purpose of this section is to find the solution curve in regions far from the singular point s_2. Let us consider again the exact circuit equations:

$$\frac{di_L}{d\tau} = I - Ki_L - i \quad ; \quad \frac{di}{d\tau} = i_L - \phi(i) \quad .$$

We can approximate the characteristic curve around point Q with

$$\phi(i) \cong i_{L1} + \frac{1}{k}(i - i_1)$$

within a certain region $i_1 - \delta_1 < i < i_1 + \delta_2$. Substitution of $\phi(i)$ into the differential equation yields

$$\frac{di_L}{d\tau} = I - Ki_L - i \quad ; \quad \frac{di}{d\tau} = i_L - i_{L1} - \frac{1}{k}(i - i_1) \quad .$$

Equating to zero and solving, we determine the singular point s_1. Graphically, s_1 is the intersection of the load line with the tangent to the characteristic curve at Q_1. Point s_1 is virtual because it falls out of the region under consideration. Moving the origin of coordinates to s_1, we obtain

$$\frac{dh_1}{d\tau} = - Kh_1 - h_2 \quad ; \quad \frac{dh_2}{d\tau} = h_1 - \frac{1}{k}h_2 \quad .$$

From Fig. 3.1.1-1 we obtain $K = 8/5$ and $k = 8/17$, so that $\lambda_1 = 1.82$; $\lambda_2 = -1.30$; $m_1 = -0.292$; and $m_2 = -3.42$. We can now plot the solution curve within the region $i_1 - \delta_1 < i < i_1 + \delta_2$. The complete solution curve, up to point s_2, is obtained by approximating the characteristic curve with a number of straight lines and dividing the plane in regions, as we did in Fig. 2.1.2-2.

3.1.2 Classification of Singular Points

We can conclude from the preceding study that each point of the characteristic curve can be classified in the way shown in Fig. 3.0-4.

Consider the eigenvalue formula

$$2\lambda_{1,2} = -\left(K + \frac{1}{k}\right) \pm \sqrt{\left(K + \frac{1}{k}\right)^2 - 4\left(\frac{K}{k} + 1\right)}$$

for the RCLN case, where

$$K = \sqrt{\frac{C}{L}}\, R \quad ; \quad k = \sqrt{\frac{C}{L}}\, \frac{df(e_r)}{de_r} = \sqrt{\frac{C}{L}}\, r(e_r) \quad .$$

We classify now the singular points according to the values of K and $1/k$:

a) Stability: $\beta = -\left(K + \frac{1}{k}\right)$.

$K > -1/k$ implies a stable point ;

$K < -1/k$ implies an unstable point .

The border line is $K = -1/k$.

b) Type: Node - saddle point or focus.

$$\alpha = \left(K + \frac{1}{k}\right)^2 - 4\left(\frac{K}{k} + 1\right) = \left(K - \frac{1}{k}\right)^2 - 4 \quad .$$

$\left(K - \frac{1}{k}\right)^2 > 4$ implies either a node or a saddle point ;

$\left(K - \frac{1}{k}\right)^2 < 4$ implies a focus .

The border line is

$$\left(K + \frac{1}{k}\right)^2 = 4 \text{ or } K = (1/k) \pm 2 \quad .$$

c) Type: Node or saddle

$$\left(K + \frac{1}{k}\right)^2 > \left(K + \frac{1}{k}\right)^2 - 4\left(\frac{K}{k} + 1\right)$$

or

$$4\left(\frac{K}{k} + 1\right) > 0$$

implies a node, so that

$$4\left(\frac{K}{k} + 1\right) < 0$$

implies a saddle point. The border line is

$K = -k$.

The results are shown graphically in Fig. 3.1.2-1.

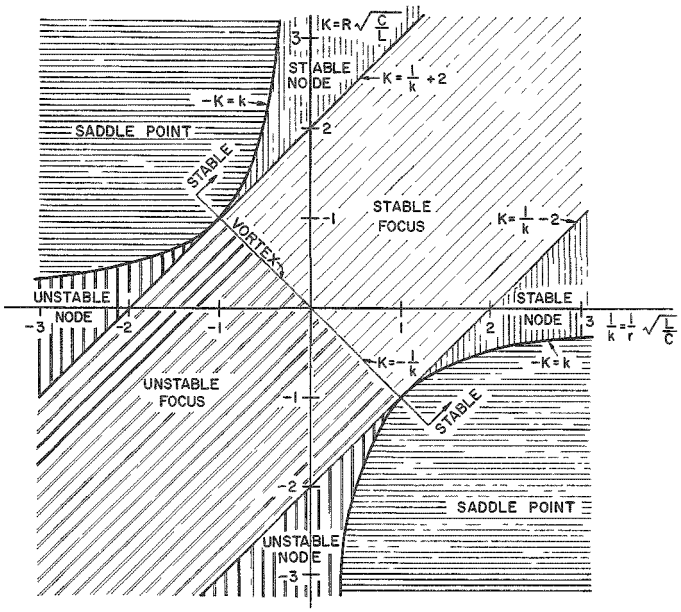

Fig. 3.1.2-1

Parameter diagram of a RCLN circuit.

Consider the first example of Section 2.3.1, in which L = 10 nhy, C = 20 pfd, and R = 2Ω. For the only real singular point,

$$r = -2.4\ \Omega\ .$$

Then

$$K = R\sqrt{C/L} = 0.09$$

and

$$\frac{1}{k} = \frac{1}{r}\sqrt{\frac{L}{C}} = -4.64\ .$$

This corresponds to an unstable node in the diagram; hence, the circuit will oscillate, as is confirmed by the analysis in Section 2.3.1. The oscillation reaches a limit cycle because the solution curve spirals into regions where 1/r becomes more positive. In the diagram, this corresponds to points on a straight line parallel to axis 1/k and to the left of the one calculated above. An equilibrium is reached when the solution curve spends part of the time in the stable focus region.

3.1.3 Operating Modes of RCLN Circuit

We have seen in previous sections that RCLN circuits can perform different functions, depending on the values of the parameters. In Section 2.3.1 we analyzed an oscillator and a binary. The mode of operation is related directly to the location of the real and virtual singular points in the diagram shown in Fig. 3.1.2-1.

To simplify the problem, we approximate the tunnel diode characteristic with four straight lines. This implies the existence of four regions (see Figs. 3.1.3-1 and Fig. 3.1.3-3). The current generator I_g and the resistance R determine whether the singular point for each region is real or virtual. The values of R, C, L, and r determine the character of the singular point and, therefore, the circuit behavior in each region.

Amplifiers and oscillators require only one real singular point in the negative region of the characteristic. In the case of the amplifier, this singularity has to be stable. Oscillators, on the other hand, require an unstable singularity. If the singularity falls in the unstable focus zone, near

the vortex line, the circuit will oscillate sinusoidally. If it falls within the unstable node zone, then we have a relaxation oscillator. The three cases are shown graphically in Fig. 3.1.3-2 (see also Fig. 3.1.2-1). The points on the horizontal dotted lines correspond to the different regions of the tunnel diode characteristic.

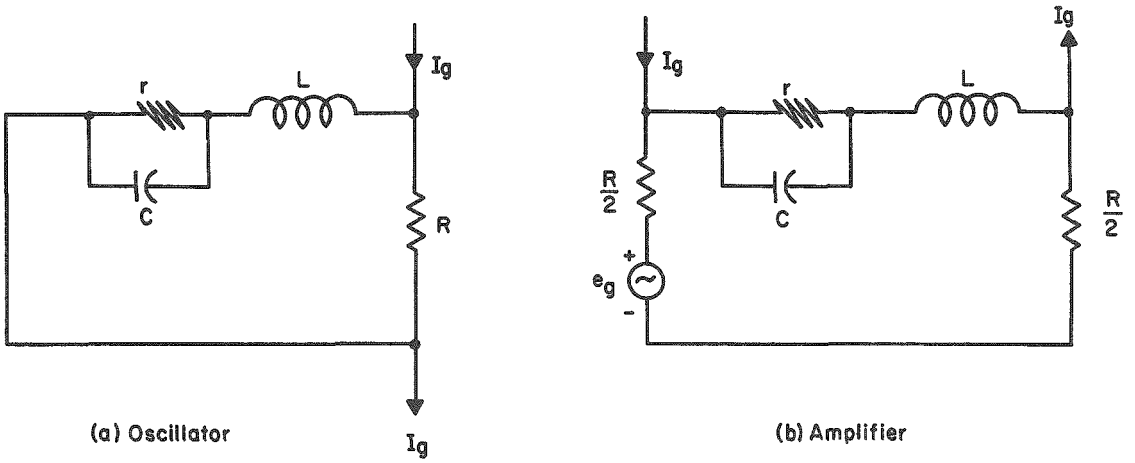

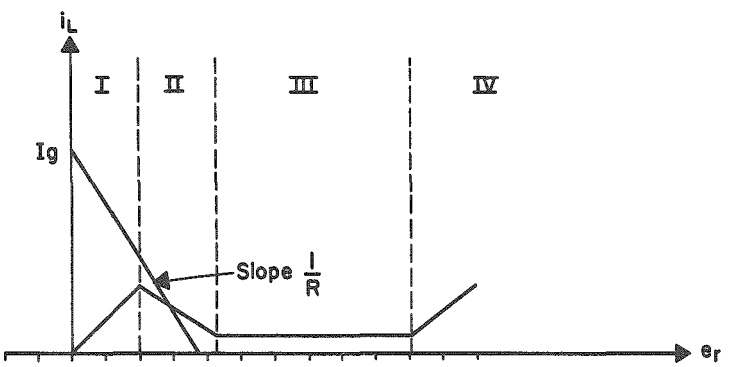

Fig. 3.1.3-1

Oscillators and amplifiers require only one real singular point in the negative resistance region.

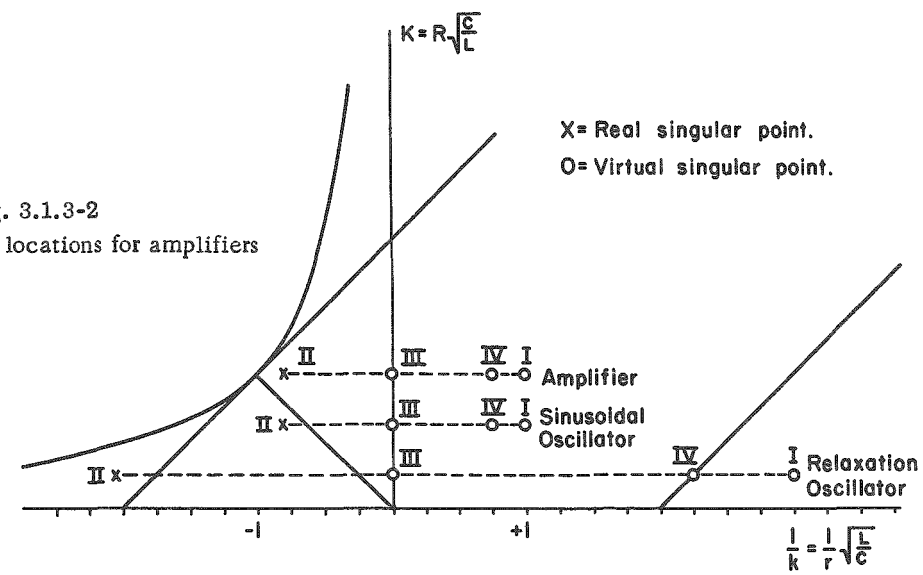

Fig. 3.1.3-2

Typical singularity locations for amplifiers and oscillators.

In the case of a bistable circuit the requirement is that $R > |r|$. The load line intersects the tunnel diode characteristic in three points, two stable and one saddle point (see Figs. 3.1.3-3 and 3.1.3-4). We see then that the diagram of Fig. 3.1.2-1 gives us a criterion for choosing the circuit parameters for each mode of operation.

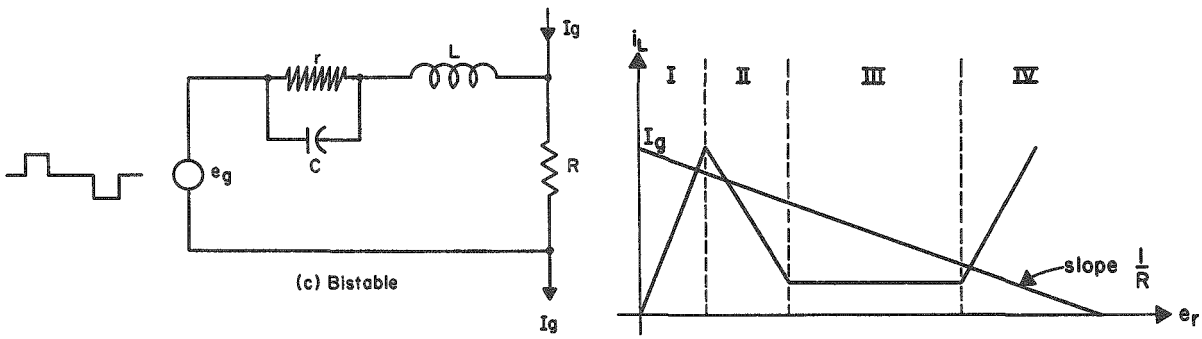

Fig. 3.1.3-3

Bistable circuit.

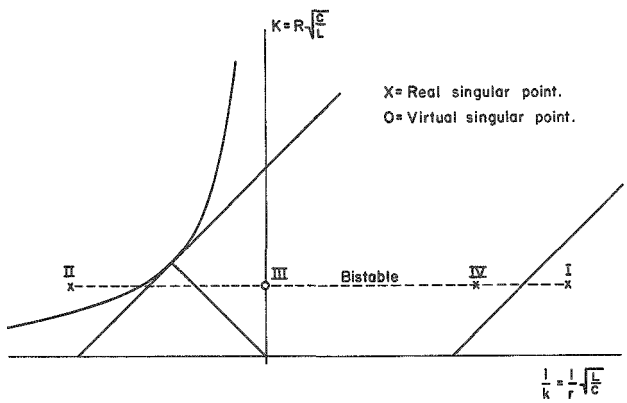

Fig. 3.1.3-4

Typical singularity locations for a bistable circuit.

3.1.4 The Goto Pair[7]

One circuit which deserves mention is that of Fig. 3.1.4-1. The circuit is a flip-flop using a Goto pair. Neglecting for the moment the capacitance present in the diodes and assuming $R_1 << R$, we have the circuit of Fig. 3.1.4-2, in which $E \cong R_1 I$. We wish to find e_1 as a function of i_1. We have

$$i_1 = i_{r_2} - i_{r_1} = f(e_{r_2}) - f(e_{r_1}) \quad ,$$

where

$$e_{r_2} = E + e_1 \quad ; \quad e_{r_1} = E - e_1 \quad .$$

Thus,

$$i_1 = f(E + e_1) - f(E - e_1) = F(e_1) \quad ,$$

as in Fig. 3.1.4-3.

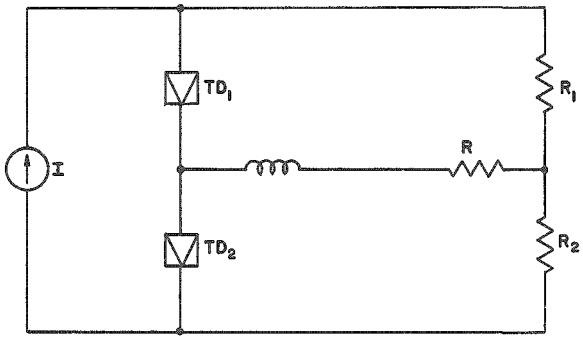

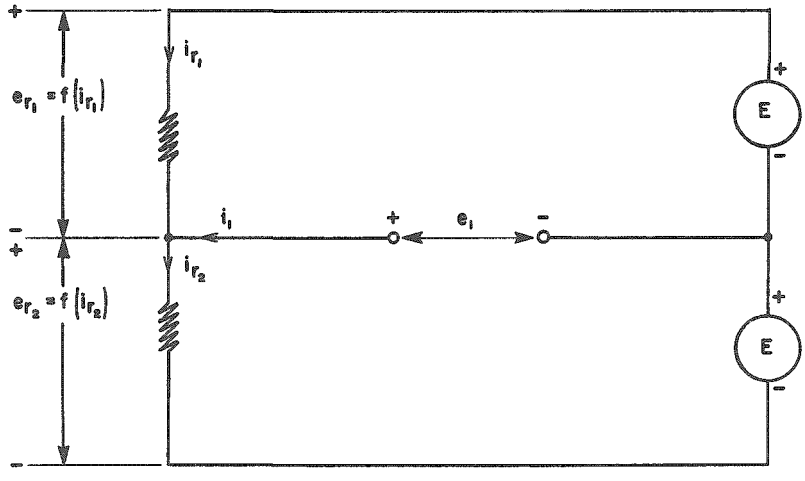

Fig. 3.1.4-2

DC equivalent circuit of a Goto pair.

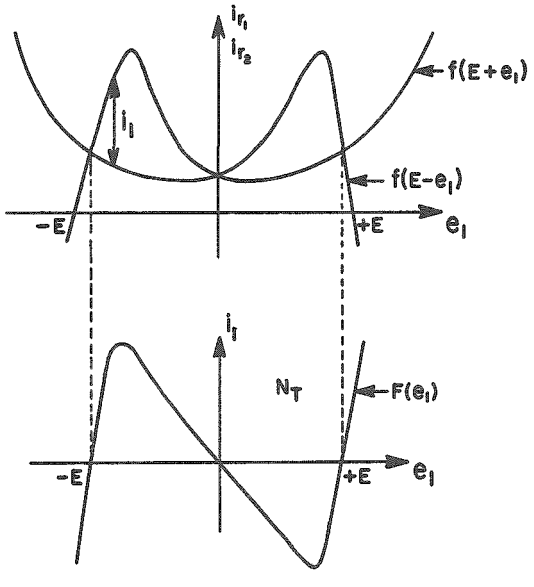

Fig. 3.1.4-3

Combined characteristic curve of a Goto pair.

Figure 3.1.4-4 shows the circuit with the capacitances included. Figure 3.1.4-5 shows an equivalent circuit, where N_T has the (i_1, e_1) characteristic found in Fig. 3.1.4-3. Given the initial conditions, we can now apply the methods used to solve a RCLN circuit.

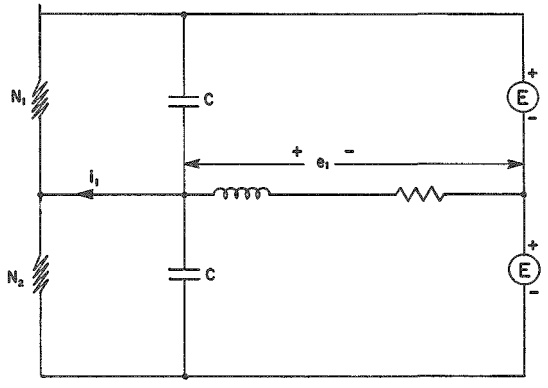

Fig. 3.1.4-4

AC equivalent circuit of a Goto pair.

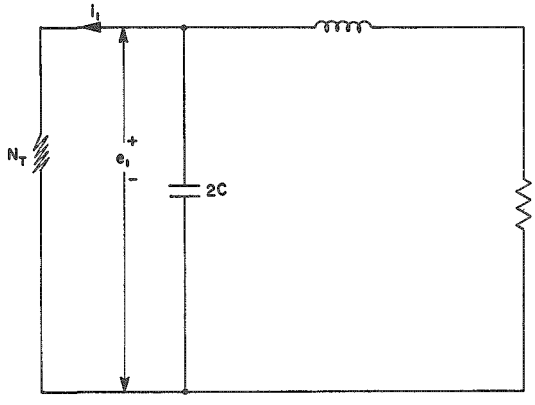

Fig. 3.1.4-5

$RCLN_T$ equivalent circuit of a Goto pair.

4. Experimental Data and Calculated Results

The methods described have been applied to actual circuits, and reasonable agreement has been obtained between calculated and observed results. The relaxation oscillator shown in Fig. 4-1 illustrates this point. The pulse generator delivers a train of rectangular voltage pulses to the input. During each pulse the load line is shifted to the negative region of the tunnel diode characteristic and the circuit oscillates. We photographed the wave forms at points A and B (with respect to ground) using a double trace-sampling scope, which was synchronized by the input pulses (see Fig. 4-2).

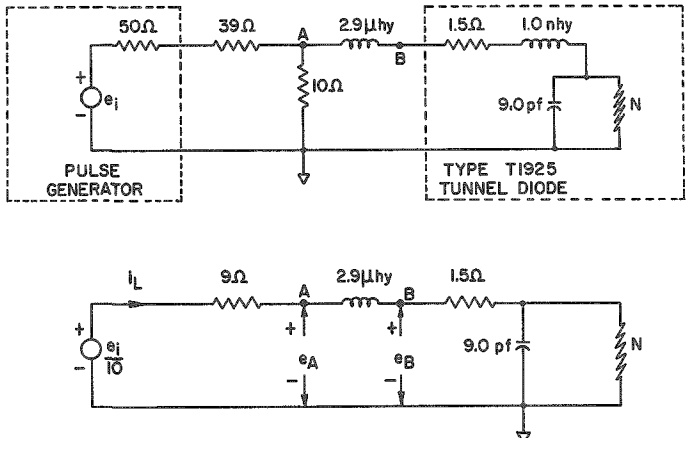

Fig. 4-1

Oscillator complete circuit and its RCLN equivalent

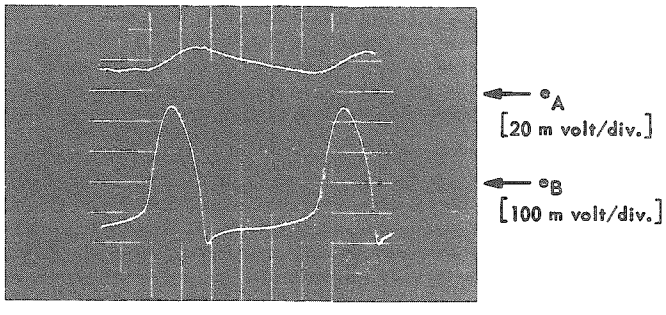

Fig. 4-2

Oscillograms of voltages e_A and e_B

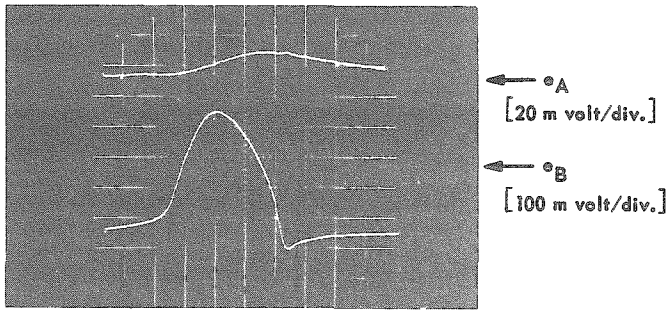

The electrical characteristics of the type T 1925 tunnel diode are:

Peak point current = I_p = 1.0 ma

Valley point current = I_v = 0.13 ma

Peak point voltage = E_p = 55 mv

Valley point voltage = E_v = 320 mv

Forward peak point current voltage = E_f = 475 mv

Total capacity = C = 9.0 pfd

Series inductance = L_s = 1.0 nhy

Series resistance = R_s = 1.5 ohms

Inflection point negative resistance = r = -120 ohms.

The tunnel diode characteristic curve is shown in Fig. 4-3. The circuit can be reduced by the Thevenin Theorem to the equivalent RCLN one

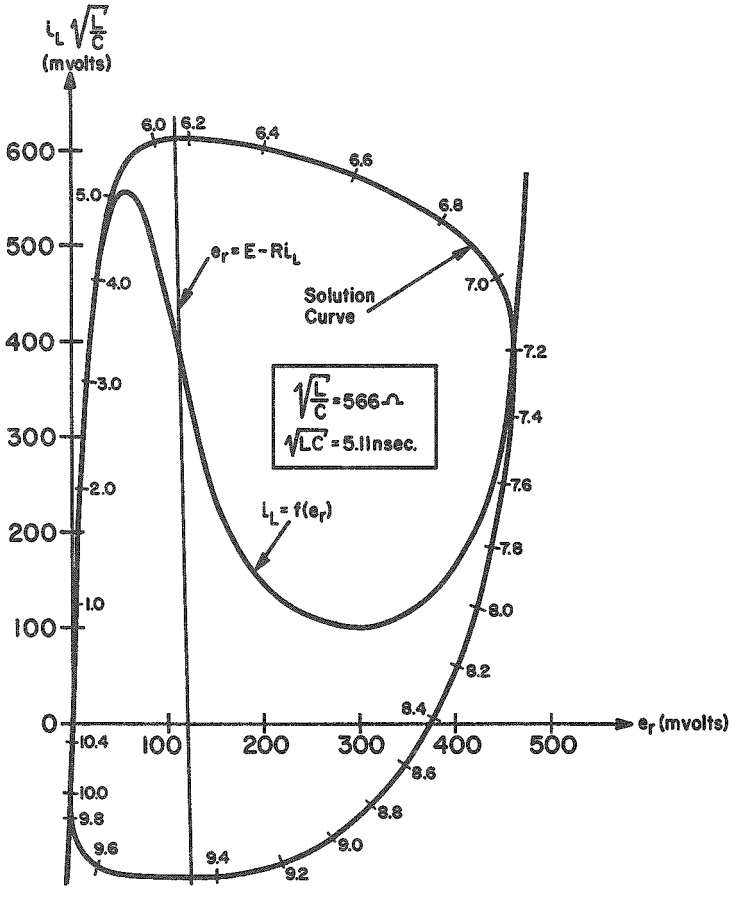

Fig. 4-3

Phase plane solution

shown in Fig. 4-1. The normalizing factors are

$$\sqrt{L/C} = 1000 \qquad \sqrt{2.9/9} \text{ ohm} = 566 \text{ ohms};$$

$$\sqrt{LC} = \sqrt{2.9 \times 9} \text{ nsec} = 5.11 \text{ nsec}.$$

The parameters K and $1/k$ are

$$K = R\sqrt{C/L} = \frac{9 + 1.5}{566} = 0.0185 \quad ;$$

$$1/k = (1/r)\sqrt{L/C} = -\frac{566}{120} = -4.72 \text{ (negative region)}.$$

The real singularity falls in the unstable node region of the parameter diagram (see Fig. 3.1.2-1).

The modified Lienard method gives the phase-plane solution curve shown in Fig. 4-3. The initial conditions for t = 0 are $e_r = 0$, $i_L = 0$, and $e_i/10 = 120$ mv. Finally, the voltage e_B as a function of time is obtained (Fig. 4-4). If we compare this wave shape with the ones obtained experimentally (see Fig. 4-2), we see that they agree reasonably well. The period of the calculated wave form is T = 54.16 nsec. This value is close to the 57 nsec observed in the photographs.

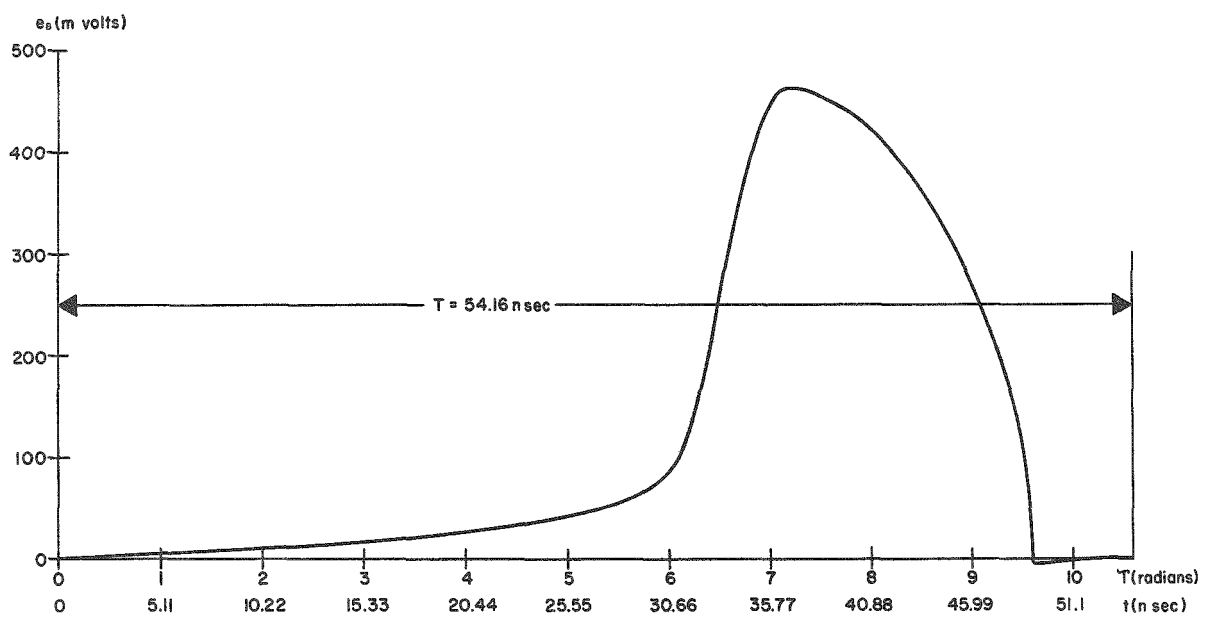

Fig. 4-4

Calculated wave form

We shall end with a few remarks.

Disagreement between experimental and theoretical results can be attributed, in our case, to the following causes:

a) The equivalent circuit of the tunnel diode is not exactly the one presented in Fig. 1.0-1

b) Some of the parameters of the equivalent circuit, for instance the capacity, are not constant and depend on the voltage e_r, on the current i_L, or on both.

c) The graphical methods, being only exact for infinitesimal increments, are intrinsically approximate.

Our feeling is that we can rule out cause a) as being minor compared with cause b). On the other hand, the equivalent circuit appears to be physically sound

Cause b) is the most serious one. It is well known[10] that the junction capacity depends on the bias e_r. If this effect is taken into account, the mathematics will be complicated excessively, making the theory too difficult to apply.

Cause c) is not too grave because it is always possible to improve the accuracy by choosing smaller increments.

Though tunnel diode circuits may be solved by means of an electronic computer,[11,12] it is believed that the simple and easily applied methods presented in this paper not only give acceptable solutions but also valuable insight into the behavior of nonlinear systems in general and tunnel diodes in particular.

ACKNOWLEDGMENTS

It is a pleasure to acknowledge the help and encouragement received from everybody related with this paper at Argonne National Laboratory. This work is part of a tunnel diode applications research project carried out in the Electronics Division with the support of the Physics and High Energy Physics Divisions.

The author is specially indebted to Robert J. Epstein and Louis J. Koester, Jr. for their advice and to David B. Gustavson for his assistance in the writing of the paper.

REFERENCES AND BIBLIOGRAPHY

1. Cunningham, W. J., Introduction to Nonlinear Analysis, McGraw-Hill Book Co., Inc., New York (1958).

2. McLachlan, N W., Ordinary Non-linear Differential Equations in Engineering and Physical Sciences, (second edition) Oxford at Clarendon Press (1956).

3. Esaki, L., New Phenomenon in Narrow Germanium p-n Junctions, Phys. Rev., 109, 603-604 (1958).

4. Lesk, I. A., Holonyak, N., Davidsohn, U. S., and Aoron, M. W., Germanium and Silicon Tunnel Diodes. Design, Operation and Application, IRE Wescon Convention Record (1959).

5. Sommers, H. S., Tunnel Diodes as High-frequency Devices, Proc. IRE, 47, 1201-1206 (July 1959).

6. Pucel, R. A., Physical Principles of the Esaki Diode and Some of Its Properties as a Circuit Element, Solid State Electronics, 1, 22-33 (1960).

7. Goto, E. et al., Esaki Diode High Speed Logical Circuits, IRE Trans. on Electronic Computers, Vol. EC-9, pp. 25-29 (March 1960).

8. Hines, M. E., High Frequency Negative-resistance Circuit Principles for Esaki Diode Applications, Bell Syst. Tech. J., 39, 477-513 (May 1960).

9. Holonyak, N., Lesk, I. A., Galium Arsenide Tunnel Diodes, Proc. IRE, 48, 1405-1409 (Aug 1960).

10. Zorky, J., Measurement of the Equivalent Circuit Parameters of Tunnel Diodes, Gen. Radio. Exp., 34, No. 7-8 (July-August 1960).

11. Kaupp, H. R., and Crosby, D. R., Calculated Waveforms for Tunnel Diode Locked Pair, Proc. IRE, 49, 146-154 (Jan 1961).

12. Schuller, M., and Gartner, W. W., Large Signal Circuit Theory for Negative-resistance Diodes, in Particular Tunnel Diodes, Proc. IRE, 49, 1268-1278 (Aug 1961).